Final Scientific/Technical Report for DoE/EERE Wind & Water Power Program

Project Title:	An Integrated Approach To Offshore Wind Energy Assessment: Great Lakes 3D Wind Experiment
Project Period:	09/30/2011-12/31/2016
Submission Date:	08/17/2017
Recipient:	Cornell University
Website:	http://www.geo.cornell.edu/eas/PeoplePlaces/Faculty/spryor/DoE_AIATOWEA/index.html
Award Number:	DE-EE0005379
Working Partners:	Clarkson University, Case Western Reserve University, SgurrEnergy, Arizona State University, EDP Renewables, RISØ DTU Wind Energy
Cost-Sharing Partners:	Clarkson University, Case Western Reserve University, SgurrEnergy, Arizona State University, RISØ DTU Wind Energy
Principal Investigators:	R.J. Barthelmie, Croll Fellow and Professor, Sibley School of Mechanical & Aerospace Engineering, Cornell University, Upson Hall, Ithaca, NY14853 (rb737@cornell.edu) S.C. Pryor, Professor, Department of Earth and Atmospheric Sciences, Cornell University, Ithaca, NY 14853 (sp2279@cornell.edu)
DOE Project Team:	DOE HQ Program Manager – Jose Zayas
	DOE Field Contract Officer – Pamela Brodie
	DOE Field Grants Management Specialist – David Welsh
	DOE Field Project Officer – Bradley Ring/Nick Johnson
	DOE/CNJV Project Monitor –Martha Amador

o *Acknowledgment*: "This material is based upon work supported by the Department of Energy, Wind Energy Technologies Office, under Award Number EE0005379.

1 Executive summary

This grant supported fundamental research into the characterization of flow parameters of relevance to the wind energy industry focused on offshore and the coastal zone. A major focus of the project was application of the latest generation of remote sensing instrumentation and also integration of measurements and numerical modeling to optimize characterization of time-evolving atmospheric flow parameters in 3-D. Our research developed a new data-constrained Wind Atlas for the Great Lakes, and developed new insights into flow parameters in heterogeneous environments. Four experiments were conducted during the project:

- At a large operating onshore wind farm in May 2012.
- At the National Renewable Energy Laboratory National Wind Technology Center (NREL NWTC) during February 2013.
- At the shoreline of Lake Erie in May 2013.
- At the Wind Energy Institute of Canada on Prince Edward Island in May 2015.

The experiment we conducted in the coastal zone of Lake Erie indicated very complex flow fields and the frequent presence of upward momentum fluxes and resulting distortion of the wind speed profile at turbine relevant heights due to swells in the Great Lakes. Additionally, our data (and modeling) indicate the frequent presence of low level jets at 600 m height over the Lake and occasions when the wind speed profile across the rotor plane may be impacted by this phenomenon. Experimental data and modeling of the fourth experiment on Prince Edward Island showed that at 10-14 m escarpment adjacent to long-overseas fetch the zone of wind speed decrease before the terrain feature and the increase at (and slightly downwind of) the escarpment is ~3–5% at turbine hub-heights.

Additionally, our measurements were used to improve methods to compute the uncertainty in lidar-derived flow properties and to optimize lidar-scanning strategies. For example, on the basis of the experimental data we collected plus those from one of our research partners we advanced a new methodology to estimate *a priori* the uncertainty in wind speed retrievals from arc scans based on site characteristics such as wind velocity, turbulence intensity and proposed scan geometry.

Insights regarding use of remote sensing technologies deriving from project experiments were used to compile a best practice document http://doi.org/10.7298/X4QV3JGF for measuring wind speeds and turbulence offshore through in-situ and remote sensing technologies.

A project-specific web-site was developed and is available at: http://www.geo.cornell.edu/eas/PeoplePlaces/Faculty/spryor/DoE_AIATOWEA/index.html

Table of contents

2 Project Overview

2.1 Objectives

Offshore and coastal wind energy developments require uniquely accurate assessments of wind and turbulence characteristics away from the surface in the marine boundary-layer. This project (which ran from 2011-2016) is a public-private collaborative between academia and industry to effectively address offshore resource assessment and design condition needs. We integrate ground-based remote sensing measurements (including multiple vertical and scanning lidar systems), observations from an Unmanned Aerial Vehicle (UAV) and a tethered balloon with in situ measurements from meteorological towers and satellite-borne radiometers to quantify horizontal/vertical gradients of both wind speed and turbulence at high temporal and spatial resolution near a large onshore wind farm, in the coastal/offshore areas of Lake Erie (in an area that has been earmarked for offshore wind farm development) and at a coastal escarpment. The datasets collected within the project are (i) linked to existing resource estimates, (ii) used in a closure (instrument inter-comparison) analysis based in part on the in situ observations, (iii) used to evaluate meteorological and wind farm models (iv) analyzed to characterize meteorological conditions in the coastal Great Lakes region where highly resolved observations are currently lacking, and (v) used to develop best-practice strategies and documentation for each measurement type focused on its application to wind energy.

2.1.1 Specific Objectives

Objective 1. To evaluate the potential of use of innovative (ground-based and satellite-borne) remote sensing technologies in offshore wind energy resource assessments.

Objective 2. To promote greater understanding of the variability of wind and turbulence in offshore and coastal areas at heights and scales and precision/accuracy of relevance to wind energy using a combination of remote sensing, in situ measurements and state-of-the-art model tools.

Objective 3. To develop a uniquely detailed and integrated dataset for model validation efforts focused on the temporal and spatial variability of potential power at turbine hub-heights and turbulence generated loads across the wind turbine rotor plane.

Objective 4. To develop instrument deployment, and data analysis and integration protocols codified in a best practice report.

2.2 Outcomes

In this project, a number of experiments were performed at full-scale to investigate how the major properties that are of interest in wind energy development offshore can be characterized using a combination of measurements (both in situ and remote sensing (ground-based and satellite-borne) and models. We worked with a number of state of the art instruments including lidars (**li**ght **d**etection **a**nd **r**anging) that measure wind and turbulence with very high precision and accuracy using a technique based on the emission and detection of aerosol movements using laser generated (eye-safe) beams. The advantage of lidar over conventional anemometers is that they measure over a volume rather than just at a point. Hence, vertically pointing Doppler lidar can measure over 10 heights to at least 200 m height in the atmosphere, while scanning Doppler lidar have the potential to describe wind speeds over several kilometers horizontally and up to 1 km vertically. In principle, the whole wind field can be accurately measured without the need for tall meteorological masts or many masts at multiple locations. While vertical lidar are now widely used in wind energy, scanning lidar can be more difficult to operate and result in large data volumes that require expert processing. Within this project we developed new methods to quantify and reduce uncertainty in flow measurements deriving from remote sensing technologies with a specific focus on scanning pulsed Doppler lidar. We also investigated new methodologies for blending data from satellite-borne instruments, in situ measurements and modeling. An example of this research is the development of a new satellite-constrained wind atlas for the Great Lakes (see details below).

Using a suite of measurement techniques we have further improved understanding of atmospheric flow parameters of relevance to the wind energy industry and wind turbine wake characteristics for wind turbine resource assessment, siting and load assessment in complex terrain.
In addition to the 14 international refereed journal papers listed below, 60 conference papers and presentations were given and a special session organized on the results of the Prince Edward Island experiment at the WindTech 2 conference held at Western University in October 2015. This project also contributed to capacity building via the training of the next generation of scientists and engineers. Two graduate students and one Post Doc participated in the project under the supervision of Professor Barthelmie and were partially supported by this project. Both students have successfully graduated with M.Eng and Ph.D. from Cornell University and one student was supported at Case Western University graduating with a M.Sc. degree.

2.2.1 Outcomes by Specific Objectives

Objective 1. To evaluate the potential of use of innovative (ground-based and satellite-borne) remote sensing technologies in offshore wind energy resource assessments.

- Research within this theme led to one of our key research products: A new Wind Atlas for the Great Lakes. The Great Lakes are increasingly the focus of discussions regarding offshore wind turbine deployments, but there remains unacceptably large uncertainty in the likely wind resource. Thus, a highly innovative approach was undertaken to develop a homogeneous wind atlas for the Great Lakes using a unique integration of remote sensing data (from QuickSCAT and Synthetic Aperture Radar), in situ measurements (from buoy and coastal masts), reanalysis products and numerical models to generate low error wind fields. The Atlas is available in digital form from the project website.
- During the project we collaborated with multiple partners in field campaigns applying lidar technologies and other state-of-the-art instrumentation to improve error quantification for measurements with scanning lidar and advance methods that can be applied to optimize lidar scan geometries. Our research developed new methodologies for characterization of and reduction of uncertainty associated with lidar retrievals of flow.
- Lastly, we also advanced new approaches to characterize wind turbine wakes using lidar measurements.

Objective 2. To promote greater understanding of the variability of wind and turbulence in offshore and coastal areas at heights and scales and precision/accuracy of relevance to wind energy using a combination of remote sensing, in situ measurements and state-of-the-art model tools.

This was the major thrust of our research. Two of our experiments (#3 and #4) addressed this issue specifically. Our research shows:

- Experimental data collected during the third experiment (conducted on the shoreline of Lake Erie near the city of Cleveland) indicated the frequent presence of upward momentum and resulting distortion of the wind speed profile at turbine relevant heights due to swells in the Great Lakes. Additionally our data (and modeling) indicate the frequent presence of low level jets at 600 m height over the Lake and occasions when the wind speed profile across the rotor plane may be impacted by this phenomenon.
- Experimental data and modeling of the fourth experiment on Prince Edward Island showed that at 10-14 m escarpment adjacent to long-overseas fetch the zone of wind speed decrease before the terrain feature and the increase at (and slightly downwind of) the escarpment is ~3–5% at turbine hub-heights. A region of high turbulence was indicated close to the escarpment that extended through the nominal rotor plane, but the horizontal extent of this region was narrow (<10 times the escarpment height, H) in both models and observations. While flow angles close to the escarpment were very complex, by a distance of 10 H, flow angles were <3° and thus well within limits indicated by design standards.

Objective 3. To develop a uniquely detailed and integrated dataset for model validation efforts focused on the temporal and spatial variability of potential power at turbine hub-heights and turbulence generated loads across the wind turbine rotor plane.

- The four experiments all contributed to our efforts in this regard, culminating in our work within Exp#4 where we developed a measurement strategy that permitted direct model validation and verification for a CFD code.
- Our work also used lidar remote sensing and in situ measurements to address a key area of research; how do large onshore wind farms impact local-regional climate? Our research demonstrated that at 2.1 km, or 26 rotor diameters (D) downstream of the closest wind turbine, but in the wake of the whole wind farm, no significant reduction of hub-height wind speed or increase in turbulence intensity (TI) was observed, especially during daytime. Thus, in high turbulence regimes even very large wind installations may have only a modest impact on down-stream flow fields. No impact is observable in daytime vertical temperature gradients at downwind distances of > 2 km, but at night the presence of the wind farm does significantly decrease the vertical gradients of temperature (though the profile remains stably stratified), largely by increasing the temperature at 2 m.

Objective 4. To develop instrument deployment, and data analysis and integration protocols codified in a best practice report.

- The return strength of a laser pulse at given distances (range gates) is dictated by the abundance of aerosols (liquid or solid particles) of a diameter approximately equal to the lidar wavelength in the sample volume. There are numerous sources of these aerosols (e.g. sea spray, dust), but the relative abundance of aerosols is spatially variable and thus the maximum range at which it is possible to retrieve robust Doppler shift information (and hence wind speeds) also varies in space. This was manifest in our field experiments. While in both the Indiana and WEICAN experiments the maximum achievable range with the Galion scanning Doppler lidar was routinely in excess of 1.5 km, very few periods during the deployment in Lake Erie exhibited valid data from this range. This we attribute to relatively low aerosol burdens associated with flow from over the lake and the relative lack of sea spray aerosols due to the low salinity of the lake and thus the evaporation of droplets in the atmosphere. Since there is a cost associated with the dwell times necessary to retrieve Doppler shift information from longer ranges we reduced the number of range gates scanned during the Lake Erie experiment in order to reduce the time for each total scan and thus allow additional elevation angles or higher resolution azimuth angles to be included. It is our recommendation that in the initial phase of scanning Doppler lidar aerosol measurements be made to assess aerosol burdens and tests be conducted to appropriately set the maximum scan range and therefore optimize the scan geometry to avoid excess dwell times and thus enhance scan density or scan at slightly higher temporal resolution.
- We have written and published a best practice report that is available for download from the project website. Citation: Barthelmie, R.J., Wang, H., Doubrawa, P. and Pryor, S.C. 2016: Best practice for measuring wind speeds and turbulence offshore through in-situ and remote sensing technologies. Report to Department of Energy. DE- EE0005379. 7 July 2016. 47 pp. The permanent URL is http://doi.org/10.7298/X4QV3JGF.
- From our Exp#1 we also published a paper in the Bulletin of the American Meteorological Society that discussed some of the challenges to, and data integration methods employing appropriate metrics for instrument closure analyses between remote sensing and in situ measurement platforms.
- From our Exp#4 we developed a methodology to integrate experiment data with CFD output for assessment of model fidelity.

2.2.2 Additional outcomes

In a broader context, we also conducted research and published papers that:

- Propose a new more accurate model for use in the standards (IEC 61400-3-1 ED1) relating to turbulence in the offshore environment (Wang et al. 2014a). In brief, we propose the following new Normal Turbulence Model for offshore wind turbine design that has the following form:

$$TI_{ONT} = \frac{\kappa[{C_{NT}}^2 + {C_{MX}}^2(-z_i/L)^{2/3}]^{1/2}}{[\ln(z/z_0) - \psi_m(z/L)]} + \Delta TI$$

σ = standard deviation of wind speed over 10 min period (m s^{-1})
C_{MX} = normalized σ in free convection layer (constant)
C_{NT} = normalized σ under neutral conditions (constant)
ΔTI = the difference between TI_{90} and <TI>
TI_{90} = the 90th percentile of *TI* for a wind speed bin
<TI> = the mean of *TI* for a wind speed bin
z = height above ground level (m)
z_0 = surface roughness length (m)
z_i = the atmospheric boundary height (m)
L = Monin–Obukhov length (m)
ψ_m function.
κ = the von Kármán constant
TI_{ONT} = the *TI* from the Offshore Normal Turbulence Model

This formulation is proposed to replace the current formulation that indicates a monotonic decay of TI with wind speed, since it better treats the two regimes of high TI – mechanically derived TI at high wind speeds and thermally derived high TI at low wind speeds. See journal article for full derivation and validation.

- Indicate that implementation of moderate wind energy scenarios can have a meaningful impact on reducing greenhouse gases emissions (Barthelmie and Pryor 2014). Scenarios from international agencies indicate that wind energy could supply 10–31% of electricity worldwide by 2050. Using these projections within Intergovernmental Panel on Climate Change Representative Concentration Pathway (RCP) climate forcing scenarios, we show that dependent on the precise RCP followed, pursuing a moderate wind energy deployment plan by 2050 delays crossing the 2°C warming threshold by 1–6 years. Using more aggressive (but still technically feasible) wind turbine deployment strategies delays 2ºC warming by 3–10 years, or in the case of RCP4.5 avoids passing this threshold altogether.
- Examine how the cost of offshore wind turbine deployments is related to factors such as the distance of the wind farm to the coast and its size (Sovacool et al. 2017). We investigated the risk of cost over-runs and under-runs occurring in the construction of 51 onshore and offshore wind farms commissioned between 2000 and 2015 in 13 countries. These projects required about $39 billion in investment and reached about 11 GW of installed capacity. Our analyses indicate there was no significant relationship between the size of a budget and the propensity for an under-run, or between the size of a wind farm in total capacity (MW) and the occurrence of a cost over-run, and only a loose relationship between average turbine size (in MW) per wind farm and the risk of an overrun. However the risk increases for larger wind farms at greater distances offshore that use new types of turbines and foundations. Although almost two thirds of the wind farms in our sample (61%) suffered from a cost over-run, the mean amount of that over-run (6.5%) was relatively minor compared to other major energy and infrastructure projects, and 20 projects (39%) actually saw construction cost as budgeted or under-runs.

See full details in the papers (full citations are given below in the Journal Publications section).

3 Experiments conducted during the project

3.1 Experimental overview

Four major experiments were conducted during the project. Table 3.1 summarizes the objectives, instruments deployed and some key references arising from each experiment. Each of the experiments investigated different specific science objectives with a common theme of improved understanding of application of lidars for characterization of flow parameters of relevance to the wind energy industry and in each the lidar deployments were supplemented with conventional equipment whose properties and error-characteristics are well-known. Three of the experimental periods were also the subject of significant numerical modeling efforts using the Weather Research and Forecasting (WRF) model and in one case the Computational Fluid Dynamics (CFD) version of the Wind Atlas Analysis and Application Program (WAsP-CFD).

Table 3.1. Précis of the major field experiments conducted under this grant

Experiment name	Date	Primary scientific objective(s)	Instruments	Numerical simulations	Additional instruments deployed by unfunded collaborators	Key References
1) Indiana wind farm	May 2012	a) Quantify spatial variability of flow across wind farm b) Quantify individual wind turbine wakes and whole wind farm wakes	G, Z×2,T, U	WRF	IEC mast *2 with cup-anemometers operated independently	(Barthelmie et al. 2014; Smith et al. 2013)
2) NREL	Jan-Mar 2013	a) Quantify uncertainty in scanning lidar estimates of flow parameters b) Optimize lidar scanning strategies for error reduction	G		IEC mast with sonic anemometers operated by NREL	(Wang et al. 2015)
3) Lake Erie	May 2013	Improve understanding of flow in the coastal zone	G, Z×3, S×2	WRF		(Wang et al. 2014b)
4) Prince Edward Island	May 2015	a) Quantify wind energy relevant flow parameters at/behind a coastal escarpment b) Quantify wind turbine wake behavior in complex coastal environments	G, Z×3, S×4	WRF, WAsP-CFD	S were deployed on an IEC mast operated by the WEICan. Short-range windscanner deployed by DTU/Western U. Multiple short-towers with cup-anemometers deployed by York U.	(Barthelmie et al. 2016; Doubrawa et al. 2016; Wang et al. 2016a)

Key to instrument abbreviations; G = Galion scanning Doppler lidar, Z = ZephIR vertically pointing continuous wave lidar, S = Sonic anemometers, T= tethersonde lifting system with 2 instrument packages, U = Unmanned Aerial Vehicle (Clarkson University) with sonic anemometer

In the following sub-sections each experiment is described in terms of the experimental design:

- Objective
- Site
- Timeline
- Instrumentation and Configuration
- Layout
- Participating institutions

Followed by major results.
For the first experiment particular effort was expended in documenting logistical aspects of the field deployment and drawing best practice recommendations, thus for this experiment there is an additional section that describes this aspects of the experiment.
The following metadata are provided for each instrument deployed in the four experiments:

- Technology
- If lidar: description of scan geometry used
- Installation
- Measurement scenario
- If lidar: description retrieval type

3.2 Experiment #1 at a wind farm in Indiana

3.2.1 Experimental description

3.2.1.1 Objective
This experiment was conducted at a large wind farm in northern Indiana and had two primary research objectives; a) Quantify spatial variability of flow across wind farm b) Quantify individual wind turbine wakes and whole wind farm wakes. An additional key objective of this experiment was to conduct detailed closure experiments for individual instruments and to develop a methodology for data integration.
3.2.1.2 Site
Experiment location = Northern Indiana wind farm (Figure 3.1). Unfortunately the operators of the wind farm requested that many of the wind farm details be removed from any materials describing the experiment, but the majority of wind turbines within the wind farm had a hub-height of 80 m, and a rotor diameter of 80-m thus we focused our sampling at this height (80 m).
3.2.1.3 Timeline
Pre-experiment testing: 7 April 2012 to 7 May 2012
Experiment period: 6 to 20 May 2012
Instrument deployment: 7 May 2012
Measurements commence: 7 May 2012
Measurements conclude: 20 May 2012
Instrument removal: 20 May 2012

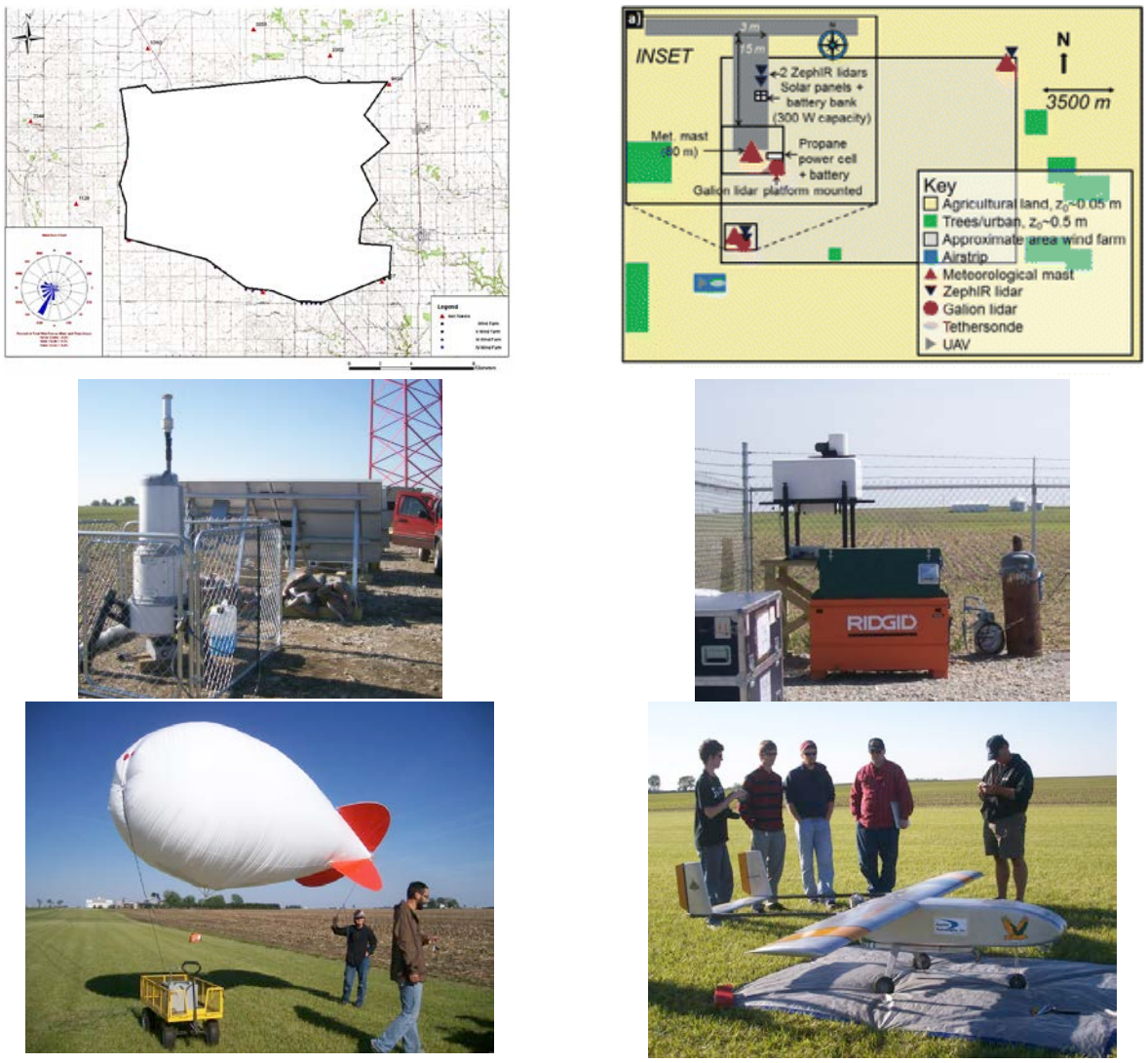

Figure 3.1 Upper panels: Illustration of the broad dimensions of wind farm (degraded at the request of the owner operator) (left) and the instrument deployed during the experiment (right). Middle row: Photographs from the experiment showing one of the ZephIRs with the independent power system (solar panel plus battery bank) and right the pulsed scanning lidar (Galion) along with the fuel cell used to supply power. Lower: tethersonde deployed for vertical profiling (left) and the Clarkson Unmanned Aerial Vehicle being prepared for flight (right).

3.2.1.4 Layout and conditions during the experiment

Unfortunately the operators of the wind farm requested the wind farm details be removed from any materials describing the experiment, but the majority of the instrumentation was deployed to the SW of the wind farm with limited additional instrumentation placed in the northeast of the wind farm (Figure 3.1). Conditions during the experiment were generally hot and dry. Precipitation was reported on only two days of the experiment at Indianapolis (the closest ASOS station) (8th and 9th May) and maximum daytime temperatures varied between 67 and 88°F. Given the instrument deployment (layout) a particular point of interest was the wind direction. Data from our measurements indicated a dominance of north-northeasterly and south-southwesterly directions (Figure 3.2).

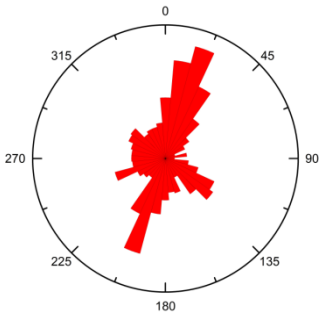

Figure 3.2 Overview of 10-minute mean wind directions during the experiment.

3.2.1.5 Instrumentation deployed and configuration

- 1×tethered balloon with instrument package for time averaged horizontal wind speed, temperature and humidity at multiple heights to height of ≤ 160 m (approx. 500 ft). The tethersonde was co-located with the UAV. Approx. 30 hours of measurements were collected in 10-min increments at 40-80-120-160 m heights using 2 measurement packages separated by ~40 m (see details in Table 3.2). Profiling was also undertaken. Note the unmanned aerial vehicle (UAV) and tethersonde were operated from a private airfield 3 km south of the main site (i.e. the southwestern corner of the wind farm.
- 3×vertically pointing continuous wave ZephIR lidars (150 series). The Natural Power's ZephIR lidar uses a continuous wave laser to determine wind characteristics from the backscatter by atmospheric aerosols. The 3 ZephIR's were operated to measure at 5 fixed heights (40, 80, 120, 160 and 200 m).
- 1×pulsed scanning Doppler lidar (Galion). A number of different scan geometries were employed (see Figure 3.3). The range-gate length was 30 m and for most scans the azimuthal spacing between beam products was < 3º with range up to a maximum of 4 km distance / 750 m height.
- 1×UAV with an Applied Technologies A series non-orthogonal ultrasonic anemometer. Horizontal and vertical transects of horizontal wind speed and turbulence. Horizontal range approx. 1 km, maximum height ≤ 300 m (approx. 1000 ft). Up to three flights per day of 20-60 minutes weather permitting. Data from the sonic anemometer along with airspeed, components of acceleration and GPS position, heading, and ground speed were collected on the Golden Eagle during 9 flights of ~20-60 minutes duration.
- One sonic anemometer that was not in the initial plan was deployed mounted on a separate 10 ft mast section at approximately 11 ft height to provide high temporal resolution measurements of momentum and heat fluxes and for determination of atmospheric stability. Despite installing surge protection the instrument was damaged by a suspected electric surge and no data were recovered.

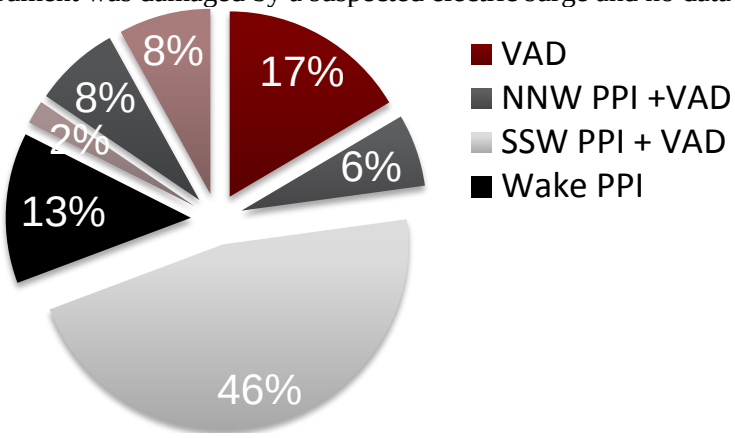

Figure 3.3 Distribution of the type of Galion scans. Explanation of terms: VAD: Velocity Azimuth Display. PPI: Plan Position Indicator. RHI: Range Height Indicator NNW and SSW indicate the central directional orientation of the PPI scans. Wake indicates a PPI scan designed to capture wind turbine wakes.

All instruments were geo-located using GPS, and all instruments were logged on computers where the time was synchronized to the atomic clock prior to the experiment start. Local standard time was used as the time coordinate as this is the time used on the meteorological masts (not Daylight Savings Time).

Table 3.2. Location and specification of instrumentation/platform (*H* = measurement height, *N* is the range of the measured parameter, *A* is accuracy, *R* is the resolution, and *U* is the uncertainty). Reproduced from (Barthelmie et al. 2014). The ZephIR units were 150 series.

Platform/ instrumentation	Owner	Measured parameters	Specifications
Meteorological mast wind sensor P2546	Wind farm operator	Wind speed	H = 80.0 m, N = 0.4–70 m s^{-1}; distance constant 1.81 m
NRG40		Wind speed	H = 60.8/41.5 m, N = 1–96 m s^{-1}, U = 0.14–0.45 m s^{-1} at 10 m s^{-1}; distance constant 2.55 m
MetOne 020C-1 and NRG200P		Direction	H = 76.0 m, N = 0°–360°, linearity < 1%
MetOne 083E-1–35		Temperature and humidity	H = 76 m, N = –50° to +50°C, A = 0.1°C, N = 0%–100%, A = ±2%
MetOne 064–2		Temperature	H = 2.5 m
MetOne 090D		Pressure	H = 76.0 m, A = 0.1 hPa, N = 600–1100 hPa, R = ±1.0 hPa over full N
Natural Power ZephIR lidar (3)	Indiana University (×2), Case Western Reserve University (1)	*u*, *v*, and *w* components of wind speed, direction, turbulence	H = 10–200 m, wind speed A = 0.5%
SgurrEnergy Galion lidar	SgurrEnergy	Wind speed	Range resolution 30 m, radial distance = 80–4000 m
Anasphere tethersonde ST5.0M, ST3.0G, ST3.0S, ST30B-15	Indiana University	Wind speed	R = 0.1 m s^{-1}, A = 1 m s^{-1} (or 5%), N = 0–59 m s^{-1}
		Wind direction	R = 1°, A = 2°
		Temperature	R = 0.125°C, A = 0.5°C, N = –55 to +125°C
		Relative humidity	R = 0.1%, A = 3%, N = 0%–100%
		Pressure	R = 0.1 hPa, A = 0.5 hPa, N = 0–1100 hPa
Applied Technologies Inc. SATI-3A	Clarkson University	Wind speed	R = 0.01 m s^{-1}, A = 0.01 m s^{-1}, N = ±65 m s^{-1}
		Wind direction	R = 0.1°, A = 0.1°
		Temperature	R = 0.01°C, A = 2°C, N = –50 to +60°C
Eagle Tree Systems Pro Recorder	Clarkson University	Aircraft speed	Airspeed: 1 m s^{-1}, GPS speed: 0.1 m s^{-1}
		Altitude	Pressure: A = 0.3 m, GPS: A = 5 m
		Position	A = 2.5 m
		Heading	A = 0.2°

3.2.1.6 Numerical simulations

To assist in the integration of different data types, WRF was run for the experiment period with 50 vertical levels, in a nested grid with lateral boundary conditions from the North American Mesoscale Model. The outer grid has 324 x 274 cells of 9 km, the inner nested grid 310 x 259 grid cells of 3 km. The physics options selected include the Mellor-Yamada-Janjic PBL scheme, and land cover was specified at a resolution of 0.7 km.

3.2.1.7 Participating institutions

Indiana University (replaced by Cornell University as the lead institution in 2014), Clarkson University, Case Western Reserve University, SgurrEnergy, Arizona State University, EDP Renewables.

3.2.2 Pre-experiment activities

Pre-experiment activities focused on:

- Evaluation of independent power supplies (fuel cell and solar panels). In the initial planning phase for the experiment the wind farm owner operators arranged to supply electrical power, but after a change of ownership this was no longer possible. Thus a range of other options were investigated:
    1. The optimal choice was two PV panels with battery storage. A larger array of 200 W to be mounted on mast 9646 by Zephyr (company approved by the wind farm owner/operator) and a smaller array of 150 W to be mounted on Mast 9636.
    2. The second choice was to use mains power available at some secondary locations such as barns near to the towers. This would have involved separate land-owner consent and agreements and was not deemed feasible due to time involved, complexity and cost of these agreements.
    3. The third choice of diesel generators. These were seen as unfeasibly noisy and/or potentially environmentally damaging.
    4. For the Galion, a very large battery bank was needed to guarantee 300 W and this was supported by a propane fuel cell that was rented from a specialist company. The propane fuel cell was very expensive and was used in the field experiment but was not affordable in the long-term.

The power supply options selected were generally found to be of good quality and the battery-charging from solar panels was readily able to maintain the correct voltage for ZephIR operation. It was further decided that the UAV and tethersonde launched from the private airfield sites would be provided with power from with separate diesel generator. Clarkson provided the diesel generator and sufficient power was available to operate the tethersonde winch and computers as well as for the UAV ground operation team. Backups included short-term battery power to allow operation of the tethersonde winch if the generator failed and a vehicle inverter was also purchased for emergency use.

- Evaluation of ZephIR lidar systems vs. mast-mounted measurements from cup (NRG) anemometers. As in the main experiment, correlation coefficients for 10-minute mean wind speeds from cup anemometers on the meteorological mast and ZephIR wind speeds were > 0.98, and a regression fit for the measurement at 80-m had an intercept of close to 0.
- A number of wind tunnel pre-experiment tests were undertaken focused on the evaluation of the integration of the sonic anemometer and associated electronics in the UAV payload bay. The tests were used to determine the extent of flow interaction with the fuselage and define the distance of the probe from the UAV fuselage to minimize flow disturbance. A custom onboard datalogger was assembled to acquire the sonic data during flight. Data was stored on an onboard micro-SD card and downloaded at the end of each individual flight.

3.2.3 Logistics consideration

3.2.3.1 Power and security considerations

- For security on site four modular 5’ by 5’ enclosures were employed, one for each lidar (see Figure 3.1). These were staked in the ground. Each enclosure had a safety sign approved by the wind farm owner/operator.
- There were no security incidents reported
- Data communication was done on site. Although the ZephIR’s should be able to communicate via modem and SIM cards these no longer work and discussions with data providers were not able to resolve the issue.
- The UAV signal did not interfere with remote access to the mast data by the wind farm owner/operator. However, there was an issue with interference between the tethersonde radio frequency and the UAV that needed to be addressed before the next experiment.

3.2.3.2 Agreements

- Memorandum of understanding was signed between all partners to indicate each group retains liability for its own instruments and equipment
- Land owner agreements had to be developed despite using only turbine access roads. Nominal payments were associated with this. An additional agreement was signed with the owner of the private airstrip.
- Non-disclosure agreement was signed between all partners. This agreement covers the use of data from the experiment.

3.2.3.3 Training, safety and access

- The wind farm owner/operator requested no work was done on site outside of normal working hours Monday to Friday without explicit permission. We did occasionally work outside of normal working hours, mainly due to weather constraints by the wind farm operators were informed and agreed to this.
- We checked in every day at the wind farm owner/operator office and every person working on the wind farm signed and adhered to the wind farm owner/operator agreement regarding safety and behavior
- Every person at the experiment attended briefings regarding behavior at the wind farm
- Every person working on the UAV activity was briefed separately on safety by Clarkson
- Every person conformed to the wind farm owner/operator rules while on site by wearing a hard hat and glasses. Each group provided their own safety equipment, plus additional fire extinguishers and weather radios
- IU supplied safety signs that the wind farm owner/operator approved for the four security enclosures
- IU supplied a list approved by the wind farm owner/operator for safety requirements in terms of first aid kits and fire extinguishers for each vehicle on site
- Vehicle access to the site was limited
- No incidents were reported

3.2.3.4 Environmental Assessment

- As described in the Experimental Design Report submitted to DoE no issues were anticipated and none occurred. Most equipment was operated on wind farm access roads and no adverse impacts were reported.
- Operation of the UAV and tethersonde undertaken with the permission of a private landing strip owner and approval from ATC in Indianapolis and proceeded without problems.

3.2.4 Major results

The first week of the campaign we experienced flow from the NW (Figure 3.2). Thus we focused the initial scans with the scanning doppler lidar on making measurements suitable for characterization of wind turbine wakes, and analysis of other instrumentation on wake characterization from the full wind farm and individual turbines. When the wind direction switched to the SW in the last few days of the campaign we focused the scanning lidar strategy on the freestream and scanning geometries to maximize the overlap with the tethersonde and UAV. As shown in Figure 3.3 this resulted in a large number of different scanning geometries which made subsequent processing and data comparison more difficult. This was one of several lessons learned from Experiment #1 which improved and informed Experiment #3 in the Cleveland offshore area. First, the 3D scanning lidar group has found that small degree PPI's (< 15 degree) are of less value than wider PPI scans. Previous post-processing work on other types of 3D scanning Doppler lidar must be adapted to the Galion hardware and data. Secondly, the high level (80 degrees) VAD scan was more effective in comparison studies with the tower and profilers than 50 degree VAD scans. Consequently, we used for the next study, a stack of 5 or 6 PPI's with approximately 90 degree arc-width, followed by a VAD scan with a high elevation angle, and a slow RHI roughly into the

mean wind direction (to reveal detailed vertical structure). Thirdly, changing the scanning geometry frequently makes it difficult to process and compare the data over the experiment.

The 3D Wind experiment was designed to evaluate innovative remote sensing and in situ platforms for measurements of wind and turbulence regimes in the lowest 200 m of the ABL. Results from this experiment show that both types of lidars (vertically pointing continuous wave and Doppler scanning pulsed lidars) exhibit very close agreement with collocated cup anemometers at heights extending across the rotor plane of the current generation wind turbines (i.e., Pearson correlation coefficient $r \geq 0.89$ and a high degree of linearity in response to varying wind speed). Data from cup anemometers deployed on a tethered balloon also exhibited $r \geq 0.8$ with the closest lidars and MM-mounted cup anemometers. Thus, while there remain some discrepancies between wind speed datasets from these instruments, the degree of accord is sufficient to remain cautiously optimistic (Barthelmie et al. 2014).

Datasets deriving from experiments such as the one described herein offer a range of opportunities for exploring fundamental questions pertaining to wind regimes within 200 m of the surface. For example, the degree of agreement between wind speeds as simulated by WRF in a 3 km × 3 km grid cell containing the primary measurement site indicates that for these simulations (using the Mellor–Yamada–Janjic PBL scheme and the USGS land cover classification), the destabilization of the nocturnal stable layer was delayed in WRF relative to the observations, leading to decreased correlation. Further, wind speeds at 80 m as simulated with WRF were, on average, lower than the measurements. This finding is consistent with results from previous applications to the marine PBL but is in contrast to comparison conducted relative to wind profilers in Japan, which found a positive bias throughout the lowest 1000 m for all PBL schemes tested within WRF (Barthelmie et al. 2014).

Observations of wakes using the lidars (vertically pointing and scanning) and from mast-deployed anemometers indicate that directly downstream of a turbine (at a distance of 190 m, or 2.4 rotor diameters (D)), there is a clear impact on wind speed and turbulence intensity (TI) throughout the rotor swept area. However, at a downwind distance of 2.1 km (26 D downstream of the closest wind turbine) the wake of the whole wind farm is not evident. There is no significant reduction of hub-height wind speed or increase in TI especially during daytime. Thus, in high turbulence regimes even very large wind installations may have only a modest impact on downstream flow fields. No impact is observable in daytime vertical potential temperature gradients at downwind distances of > 2 km, but at night the presence of the wind farm does significantly decrease the vertical gradients of potential temperature (though the profile remains stably stratified), largely by increasing the temperature at 2 m. Our results thus imply that at land-based wind farms wake recovery is very rapid (Smith et al. 2013).

3.2.5 Publications and presentations

Barthelmie, R.J., Crippa, P., Wang, H., Smith, C.M., Krishnamurthy, R., Choukulkar, A., Calhoun, R., Valyou, D., Marzocca, P., Matthiesen, D., Brown, G. and Pryor, S.C. 2014: 3D wind and turbulence characteristics of the atmospheric boundary-layer. *Bulletin of the American Meteorological Society*, **95**, 743–756

Smith, C.M., Barthelmie, R.J. and Pryor, S.C. 2013: In situ observations of the influence of a large onshore wind farm on near-surface temperature, turbulence and wind speed profiles. *Environmental Research Letters*, **8,** 034006 doi:10.1088/1748-9326/8/3/034006

Wang, H. and Barthelmie, R.J. 2015: Wind turbine wake detection with a single Doppler wind lidar, *Wake Conference*, Visby, Sweden, 9-10 June 2015. 9 pp. Journal of Physics: Conference Series **625** 012017 doi:10.1088/1742-6596/625/1/012017

Barthelmie, R.J., Wang, H. and Pryor, S.C. 2014: Measuring full scale wind turbine wakes, *European Wind Energy Association Conference*, Barcelona, March 2014.

Barthelmie, R.J., Pryor, S.C. and Wang, H. 2013: 3D Wind: Quantifying wind and turbulence intensity. *American Geophysical Union Fall Meeting*, San Francisco, 9-13 December 2013 (Poster A13G-0309).

Barthelmie, R.J., Wang, H. and Pryor, S.C. 2013: Wind resource and wakes - results from the 3D wind experiment. *European Offshore Wind Energy Conference and Exhibition*, Frankfurt, November 2013.

Barthelmie, R.J., S.C. Pryor, C.M. Smith, P. Crippa, H. Wang, Krishnamurthy, R., R. Calhoun, D. Valyou, Marzocca, P., Matthiesen, D. and N. Capaldo 2012: Great Lakes 3D wind experiment. Part I. Calibration and testing. *AWEA Offshore* 9-11 October 2012 Virginia Beach. (Poster).

3.3 Experiment #2 at NREL

3.3.1 Experimental description

3.3.1.1 Objective

Introduction of new measurement technologies (including lidar) requires careful performance assessment (accuracy, reliability and precision), robust uncertainty quantification and development of normative guidance (e.g. IEC 61400-12-1 protocols). It further requires development of expertise in the operation of lidar and analysis and processing of the resulting data. Some kinds of lidar are already in standard use, but use of remote sensing technologies to provide high-quality observations of relevant flow parameters in inhomogeneous terrain and/or complex forested terrain is not straightforward. There are a number of challenges to application of lidars to characterizing flow in complex environments. Notable among these is that the lidar sampled volume may be inhomogeneous. For scanning lidar there are two additional challenges: (i) difficulty in translating radial or line of sight wind speeds to the horizontal and vertical components of flow, and (ii) under-sampling of a rapidly varying flow field. Each data point comprises an average of many laser returns within a 3-second interval but each point in space is associated with a different time, and each point in space is sampled relatively infrequently. Thus there is a need to optimize scanning strategies to quantify and minimize the uncertainty in derived flow parameters. The experiment conducted at NREL was designed with these motivations and had two primary objectives:

a) Quantify uncertainty in scanning lidar estimates of flow parameters

b) Optimize lidar scanning strategies for error reduction in complex terrain.

3.3.1.2 Site

Operation of the scanning lidar in complex terrain and performance characterization with sonic anemometers was conducted at the National Wind Technology Center (NWTC) in Colorado. This site itself is relatively flat but the foothills of the Colorado Front Range are 5 km to the west introducing complex flow from this direction. On the northern edge of the site there is a building complex, and on the eastern edge there is a row of installed wind turbines. Measurements on a 134-m meteorological tower (denoted as M5) installed approximately 150 m west of the wind turbines were used to evaluate lidar performance (Figure 3.4).

3.3.1.3 Timeline

The experiment was conducted between February 15–25, 2013.

3.3.1.4 Instrumentation deployed and configuration

Sonic anemometers (sample rate 20 Hz) used in this experiment are mounted at 6 heights on long booms (boom length-to-face-width ratio = 5.7) oriented 278° clockwise from the north on a meteorological mast (M5). High-frequency measurements were flagged as missing if they were beyond the valid data range (± 30 m s^{-1}). Two types of cup anemometers were mounted on short booms (boom length to face width ratio = 2.8) attached to M5 at multiple heights and orientated 278° clockwise from the north. The Galion G-4000 pulsed Doppler lidar, distributed by SgurrEnergy, was deployed approximately 350 m west of M5. The arc scan used for the scanning lidar in this experiment has range gate size of 30 m and the elevation angle is 12.7 deg (ϕ = 12.7°). The center of the arc at range gate 11 close to the sonic anemometer at 74 m height on a meteorological mast at 350 m distance. The lidar scanning geometry was set with seven azimuth angles from 55.8° to 85.8° (i.e. $\Delta\theta$ = 30°) with a 5° interval (i.e. $\delta\theta$ = 5°). There are 25–28 radial velocity measurements per range gate over 10 minutes.

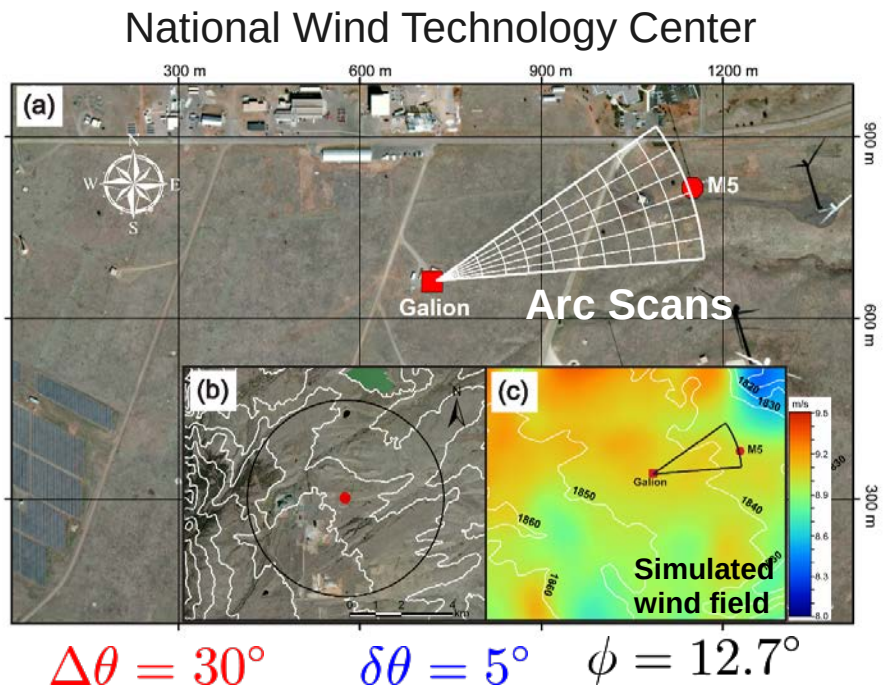

Figure 3.4 Overview of the NREL-NWTC experimental site. (a) Layout of the test site at the NWTC. The Galion lidar location is denoted by the red square, and the red circle denotes the M5. The distance between the lidar and M5 is approximately 150 m. The locations of the lidar range gates are depicted by the circular grids between M5 and the Galion. (b) The inset shows the topography surrounding the site. The interval of the overlaid elevation contour lines (white) is 50 m. The radius of the dark circle is 3.7 km, within which uniform terrain is required for horizontally homogeneous flow. (c) The inset shows the wind speed spatial distribution simulated by WAsP Engineering and the elevation contour lines (white lines and 10-m interval) derived from Shuttle Radar Topography Mission elevation data. This WAsP Engineering simulation is based on a wind speed of 9 m s^{-1} and a wind direction of 272° at a height of 74 m at the location of M5.

3.3.1.5 Participating institutions

Indiana University (replaced by Cornell University as the lead institution in 2014), and NREL.

3.3.2 Major results

Our analyses of data we collected at NREL NTWC demonstrated that for wind speeds up to 18 ms^{-1}, the slope of a regression line between 10-minute mean wind speeds retrieved from a single 30° arc scan ($\Delta\theta$) with the scanning lidar and those from a sonic anemometer was 1.033 and that the lidar estimates exhibited a root mean square error of 0.72 ms^{-1}. Uncertainties in the retrieved wind velocity from the scanning Doppler lidar are related to high turbulent wind fluctuations and an inhomogeneous horizontal wind field. The standard error of the retrieved wind speed can be minimized by increasing the azimuthal range to 5–7 azimuth angles. This research was key to subsequent research experiments in the project in terms of defining efficient and effective scanning patterns for scanning Doppler lidar and developing tools to quantify the uncertainty in its operation.

Subsequent to our deployment at NTWC we obtained scanning lidar data from three additional sites of varying terrain complexity and analyzed them along with a theoretical model in order to compute the relative importance of various parameters in determining the lidar-retrieved wind speed uncertainty and also to develop insights into the error in predicted annual energy production estimates assuming they were derived from lidar arc scans. Our results indicate:

- The uncertainty in lidar retrieved wind speeds can be scaled with the turbulence intensity.

- The lowest uncertainty can be achieved by aligning the line of sight with the wind direction. The highest uncertainty occurs when the wind direction is 45◦ relative to the line of sight.
- The uncertainty can generally be reduced by increasing arc span and decreasing beam number, although a minimum number of beams is required to characterize the wind velocity.
- If the relative angle (i.e. difference between line-of-sight and wind direction) is close to zero, adjusting scan geometry will not change the uncertainty significantly. With orthogonal scans, the uncertainty is more sensitive to beam number than arc span.
- When arc scans with a scanning Doppler lidar are used for wind resource assessment, the uncertainty in annual energy production prediction arising from uncertainty in arc scan velocity retrieval is negligible. The uncertainty decreases with decreasing surface roughness and turbulence intensity, and increasing arc span.

On the basis of the experimental data we collected and analyzed we advanced a new methodology to estimate *a priori* the uncertainty in wind speed retrievals from arc scans based on site characteristics such as wind velocity, turbulence intensity and proposed scan geometry (Wang et al. 2016b).

3.3.3 Publications and presentations

Wang, H., Barthelmie, R.J., Pryor, S.C. and Brown, G. 2016: Lidar arc scan uncertainty reduction through scanning geometry optimization, *Atmospheric Measurement Techniques*, 9, 1653–1669.

Wang, H., Barthelmie R.J., Clifton, A. and Pryor S.C. 2015: Wind Measurements from Arc Scans With Doppler Wind Lidar, *Journal of Atmospheric and Oceanic Technology*, **32**, 2024-2040.

3.4 Experiment #3 in the coastal zone of Lake Erie

3.4.1 Experimental description

3.4.1.1 Objective

As wind energy develops offshore in the United States, there is a need for techniques to quantify wind characteristics at potential sites so that power output and turbine loading can be quantified. There are many aspects of the offshore wind resource that are poorly understood and it is very challenging to make and interpret offshore measurements. Thus, there is a need for ongoing research on the use of these and other remote sensing instruments, in combination with other instruments and models, to fully characterize the properties of the atmospheric boundary-layer (lowest few hundred meters of the atmosphere). This experiment was designed to quantify wind and turbulence in the coastal zone. The site selected was to some degree chosen to be coincident with a site selected by U.S. Department of Energy to be one of seven proposals (Northeast Ohio's Project Icebreaker) to prove the promise of offshore wind power, and thus to provide insights into flow characteristics of interest to that demonstration project.

3.4.1.2 Site

Three primary sites were used in this experiment located in or just offshore of the city of Cleveland (Figure 3.5-3.10).

3.4.1.3 Timeline

Table 3.3 Experiment timetable: Experiment period: 6 - 26 May 2013

	Installation	Operation	Removal
Crib	2 May	May-August	29 August – 6 September
Port	7 May	7-24 May	24 May
Edgewater Yacht Club	8 May	8-23 May	23 May

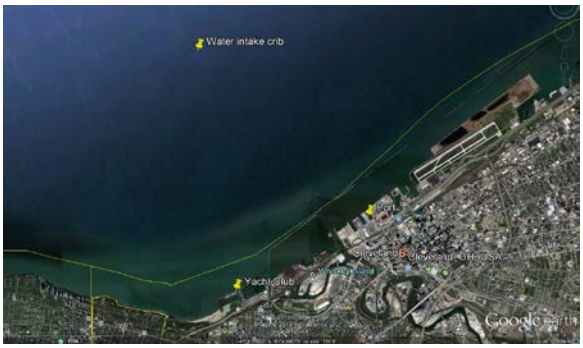

Figure 3.5 Location of the three primary measurement sites.

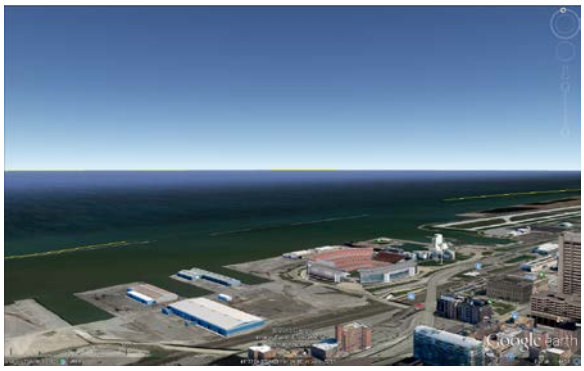

Figure 3.6 View of Cleveland Port

Figure 3.7 Photograph of water inlet crib from near the yacht club.

Figure 3.8 Photograph of the Metek sonic anemometer deployed at the Port showing the offshore fetch.

Figure 3.9 Photograph of the scanning doppler lidar (Galion) and vertically pointing lidar deployed at the Port

Figure 3.10 Photograph of the ZephIR at the water intake crib (operated by Case Western Reserve).

3.4.1.4 Layout and conditions during the experiment

Table 3.4 Experimental sites

Site	Instruments	Information regarding siting considerations
Water intake crib Continuous measurements	ZephIR unit # 160 (150 series). Gill Sonic anemometer and laptop Ongoing meteorological mast	Installed between 29 April and 5 May and removed in late August 2013 Independent power supply is not needed in short-term. Permission had to be obtained and various agencies involved in the installation of lidar and sonic on the crib, in addition to pre-experiment testing of instruments.
Port Continuous measurements	Galion (300 W) ZephIR lidar unit # 128 (150 series). Metek sonic anemometer and laptop	Limited access in secure port site. Permission obtained for installation and removal as well as one short access period per day. Pre-deployment instrument testing and power and security measures needed.
Port Other	UAV intended	It is a good open site but very close to two airports and we were unable to get UAV flight permission or permission to launch a tethersonde at this site.
Yacht Club (by Edgewater Park) Continuous measurements	ZephIR lidar unit # 127 (150 series)	Good secure location that triangulates crib and port sites.

Note: Distance from the Yacht club to water intake crib is approx. 4.8 km. Distance from the Port to crib is approx. 4.7 km.

3.4.1.5 Instrumentation deployed and configuration

Instrumentation suite deployed (see also Table 3.5) included:

- 3×vertically scanning ZephIR lidars (all series 150 units). Profiles of 10-minute mean horizontal wind speed and direction and turbulence intensity to a height ≤ 200 m at 5 heights (40, 80, 120, 160, 200 m). Note: The wind directions from the crib are severely compromised by the crib structure.
- 1×horizontally scanning Galion lidar. Range-height profiles of horizontal wind speed and turbulence to a horizontal distance of approximately 2 km and a height of 700 m. Single scan geometry employed during experiment. PPI scans with EL: 2, 4, 6, 8, 10, 20. AZ: 233:3:323°. VAD with EL: 56° AZ: 0:30:330. 67 range gates for a maximum range of 2 km.
- Meteorological mast mounted on the water intake crib. This equipment is permanently mounted.
- One sonic anemometer to be mounted on a separate 3 m mast section at the crib at approximately 11 ft height to provide high temporal resolution measurements of momentum and heat fluxes for determination of atmospheric stability.
- One sonic anemometer to be mounted on a separate 3 ft mast section at the port at approximately 3 ft height to provide high temporal resolution measurements of momentum and heat fluxes for determination of atmospheric stability.

All measurements were recorded on Eastern Standard Time that is UTC-5.

The experimental design focused on high quality measurements from lidar and data integration across a range of temporal and spatial scales to quantify the flow in 3D. The experiment encountered a number of problems - as with the experiment in Indiana the ASU scanning Doppler lidar was not available, plus the Clarkson team were not given permission to fly the UAV near Cleveland.

Table 3.5 Instrument deployment details

Location	Instrument	Height	Height (m)	File naming	GPS
Port	Galion	Ground plus table	1.5 m above ground, add 1.2 m above sea level	Start time	41°30'26.58"N, 81°42'11.51"W UTM E 441348.4m N 4595235.3m Elevation 577 ft
	ZephIR 128	Ground	2 m above ground, add 1.2	Beginning of	

	(150 series unit)		m above sea level	period	
	Metek sonic anemometer	Ground	4.14 m above ground, sea surface is 1.21 m below ground height	Start of hour	41°30”26.9’N, 81°42”12.6’W
Yacht Club	ZephIR 127	Ground plus roof	4.25 m + 2 m	Beginning of period	41°29'31.24"N, 81°43'59.59"W UTM E 438731.4m N 4593747.1 m Elevation 580 ft
Crib	ZephIR 160	Bottom platform	5.5 m above sea level plus 2 m	Beginning of period	41º 32’ 08.53’’N, 81º 44’ 37.85’’W UTM E 437954.5 m N 4598494.9 m Elevation 526 ft Water depth 16.15 m
	Gill sonic anemometer (WindMasterPro)	Top Platform	3.7 m height from top platform Gill height above water level at crib: 19.08m		

3.4.1.6 Participating institutions

Indiana University (replaced by Cornell University as the lead institution in 2014), Case Western Reserve University and Clarkson University.

3.4.1.7 Numerical Simulations

The WRF simulations were undertaken with WRF v3.5 and employed both a both nest and a triple nest configuration (Figure 3.11). Although not part of the work we originally proposed we also sought to integrate the data with very high-resolution simulations from the Weather Research and Forecasting model (WRF). This is extremely challenging due to the complexity of wind-wave interactions and coastal zone effects from Cleveland. Thus, in our analysis we only included output from the double-nested simulations. The simulation configuration is as follows:

- The center of the domain at Cleveland.
- Outer domain over entire east North America (or nearly so) at 4 km. Lower left corner at 28 N and 100 W, and the upper right at 55N 60W. Inner domain centered comprising approx.. one third of the length of the outer domain
- 70 vertical levels
- Simulation period: 6 – 27 May 2013.
- Output every 10 minutes.
- Lateral boundary conditions from NAM at 12 km

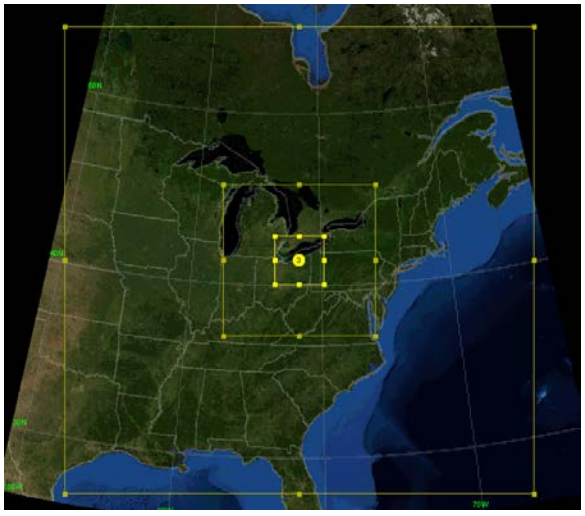

Figure 3.11 WRF domains for Cleveland experiment (domain 3 was only employed in a testing configuration).

3.4.2 Pre-experiment activities

Testing of the two sonic anemometers (one Gill, one Metek) was conducted at the Outdoor laboratory in the roof of the MSBII building on the camps of Indiana University during April 2013. Results showed relatively good agreement for 30-minute mean wind speed, direction and heat and momentum fluxes (Table 3.6). However, the Metek is noisier at higher frequencies, and it is hard to get sonic data to agree precisely in low flux conditions to better than ±20% unless they have the same head architecture (i.e. two Gill sonic anemometers should compare much better).

We also conducted inter-comparison of the two ZephIR units (unit # 127 and 128) for simultaneous measurements at five levels; z = [40, 80, 120, 160, 200]. The slopes of regression fits to the data are 0.92-0.94 for regression fits without forced zero and the R^2 values were 0.86-0.89 (Figure 3.12). These inter-comparisons thus indicate larger discrepancies than we have observed in flat terrain comparisons that may reflect highly inhomogeneous flow conditions on the roof-top laboratory.

Table 3.6 Comparison of data from the two sonic anemometers for mean values of the major variables of interest in the Cleveland field experiment (note: the mean values are from a large ensemble collected over multiple days during April 2013). The heat and momentum fluxes were computed at 30-minute integration periods

	<Wind speed> (m s^{-1})	<Wind direction> (deg)	<Heat flux> (K m s^{-1})	<Momentum flux> (m^2 s^{-2})
Gill	0.6439	164.7131	0.0671	-0.1208
Metek	0.7541	170.8840	0.0844	-0.1399

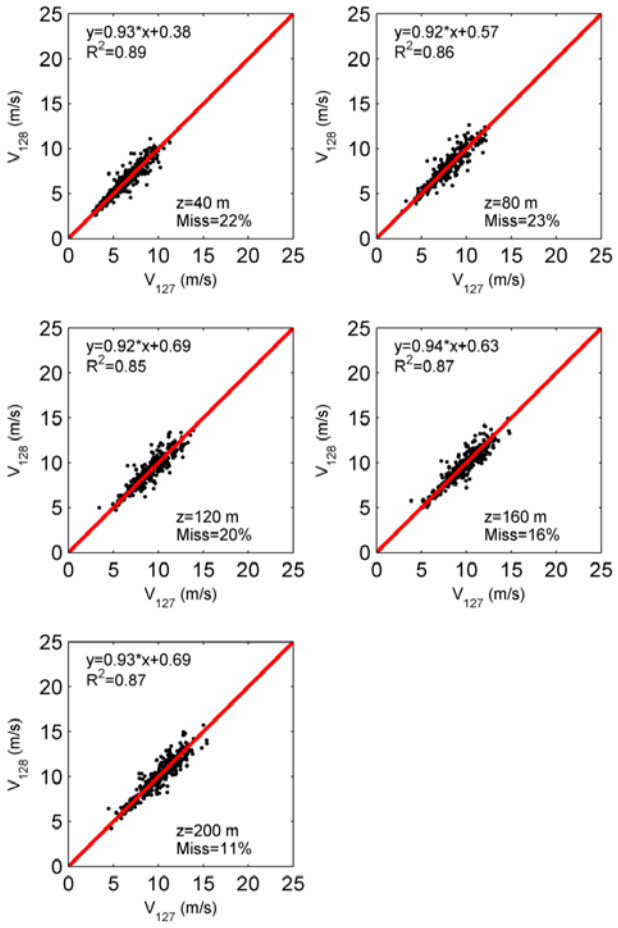

Figure 3.12 Scatterplots of wind speeds at the five measurement heights from ZephIR 127 (V_{127}) and 128 (V_{128}) in pre-experiment testing April 2013. Note missing data relates to either screening for periods of rain and or periods when the ZephIR Waltz software did not report a 10-minute mean wind speed value.

3.4.3 Major results

The major results from this experiment can be summarized:

- There are substantial gradients in wind speeds in the coastal zone and marked heterogeneity. This is illustrated by:
    - Comparisons of 10-minute wind speeds from the ZephIR units deployed on the shoreline and that on the crib, and in comparison of the sonic anemometer derived wind speeds and those from ZephIR systems (Table 3.7). As shown, while wind speeds on the crib were almost uniformly higher than those close to the shoreline, there is a relatively weak correlation in time between units on the coastline and those offshore.

Table 3.7 Regression fits to 10-minute mean wind speeds at 80 m taken with the ZephIR units. The total sample size is 1795. In the fits the first unit listed is the y-variable.

Lidar Unit	Deployment location	Range of wind speeds over that regression fit was derived	Regression fit	R^2
127 v 128	127:Yacht Club on shoreline 128: Port on shoreline	2-16 ms^{-1}	y = 0.973x + 0.211	0.87
160 v 128	160: On crib 128: Port on shoreline	2-16 ms^{-1}	y = 0.975x +1.941	0.58
160 v 127	160: On crib 127:Yacht Club on shoreline	2-16 ms^{-1}	y = 0.926x +2.223	0.57

    - Analyses of data from the scanning Doppler lidar. Offshore flow (from land to lake) accelerated up to 200 m above the surface but the degree of acceleration decreased with height (Figure 3.13, Figure 3.14). Generally, there was very low wind shear (change of wind speed with height) offshore in this environment although both the wind speed profile and the turbulence profile changed very quickly over distance from the shore
- During periods of offshore flow, the flow field at 40 m between the shoreline and crib as measured by the scanning lidar was highly complex and inhomogeneous (Figure 3.15). Further, the horizontal wind speed gradient showed the influence of atmospheric stability on flow dynamics. There was a highly non-uniform spatial wind speed distribution (~60% variation) that was enhanced when stability conditions differed between land and lake (Figure 3.15).
- Nocturnal low level jets (LLJs) were frequently observed in the Doppler lidar scans at heights between 200 and 400 m. Numerical simulations using WRF at 3 km resolution captured the occurrence of the LLJs, but its performance varied in predicting their intensity, duration, and location of the jet core (Figure 3.16 and 3.17).
- Momentum fluxes computed using data from the sonic anemometers (thus 498 hours of observations) frequently indicated upward fluxes. $F_{uw} > 0$ was observed in 35% of hours at both the Port and the Crib and of those 2/3 of hours exhibited simultaneous upward fluxes. Using data from the closest buoy in Lake Erie we found 75% of hours when the swell wave height (SWHT) exceeded 0 m, were characterized by upward momentum fluxes and when no swell wave height was reported only 15% of those hours exhibited upward momentum fluxes. Periods with multiple hours of upward fluxes were also characterized by non-ideal wind speed profiles as measured by the ZephIR lidars.

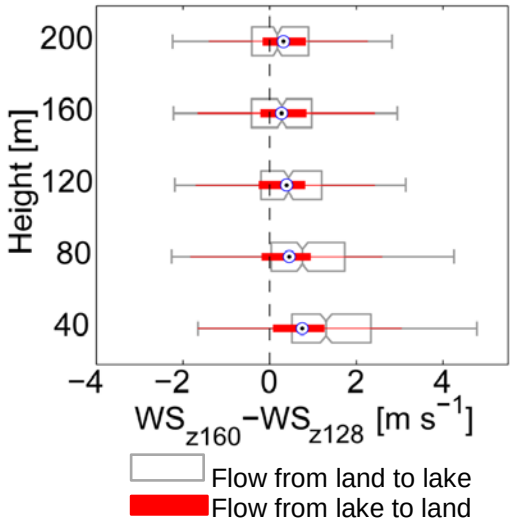

Figure 3.13 Difference between wind speeds from ZephIR units deployed on the crib (WS_{160}) – i.e. 2-3 km offshore (distance to shoreline is a function of wind direction) and the unit deployed at the port (WS_{128}) as a function of measurement height shown for offshore flow (flow from the land to the lake) and for onshore flow (flow from the lake towards the land). The differences are shown as boxplots, where the central box extends from the 25th to 75th percentile and the whiskers extend from the 1st to 99th percentile.

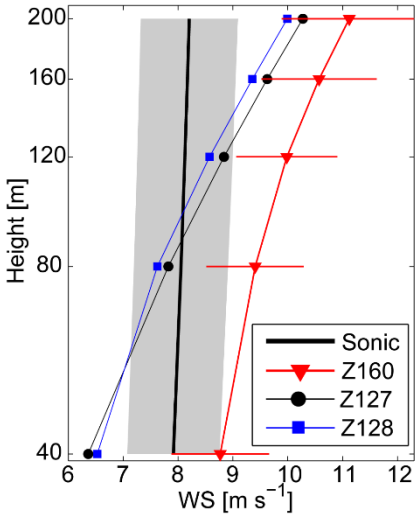

Figure 3.14 Wind speed profiles averaged between May 20, 18:00 and May 21, 09:00 during which flow was offshore and the atmosphere was unstable over the lake. The wind speed profile labeled sonic derives from measurements of wind speed from the sonic anemometer deployed at the crib and is extrapolated vertically using the Monin-Obukhov similarity theory. The profiles from the three ZephIR units are labeled according to the unit number, recall Z128 was deployed at the port, Z127 at the Yacht Club and Z160 on the crib.

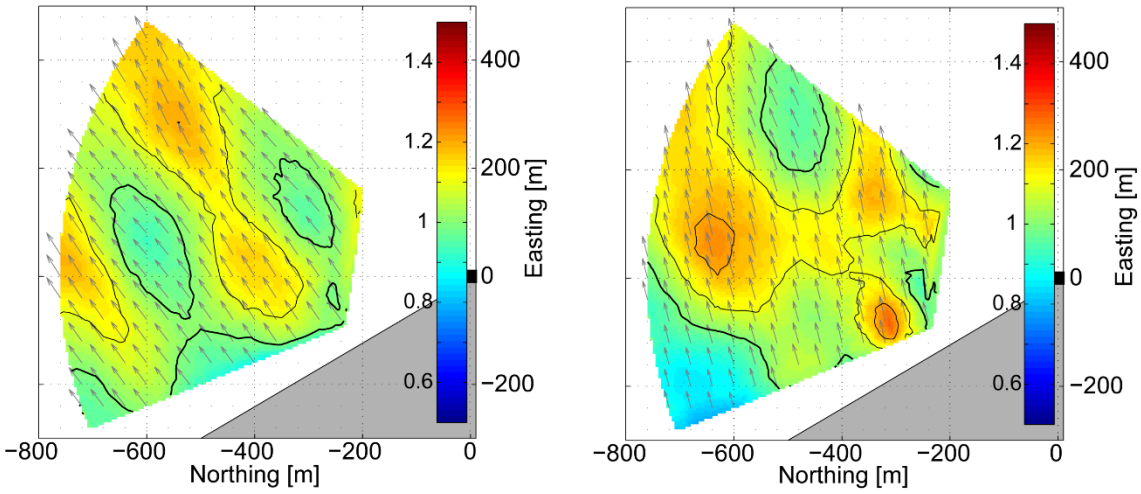

Figure 3.15 Case studies of normalized horizontal wind speed at 40 m height retrieved from Galion PPI scans for flow moving from land to lake when atmospheric conditions (a) were unstable over both the land and lake and (b) changed from being stable (over land) to unstable (over the lake). The reference wind speed from ZephIR measurements at 40 m at the port was 7.43 ms^{-1} for case (a) and 6.75 ms^{-1} for case (b). Atmospheric stability for the two cases as characterized using the Obukhov length derived from sonic measurements at the port (i.e. on land, L_{land}) and on the crib (i.e. offshore, L_{lake}) are (a) L_{land} = -53 m, L_{lake} = -3.4 m, while for case (b) they are L_{land} = -2.4 m, L_{lake} = -35 m.

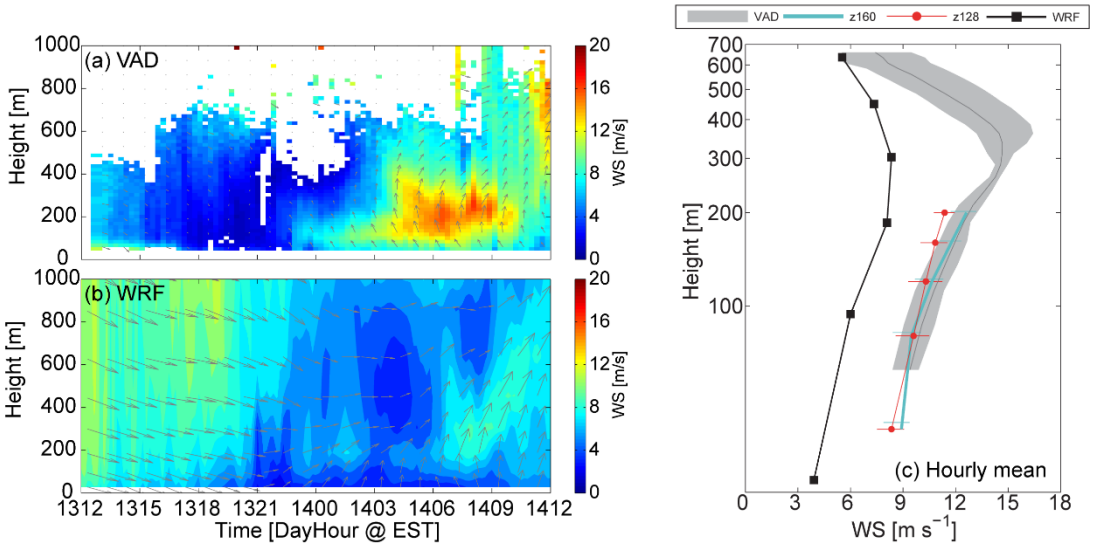

Figure 3.16 Time-height cross sections of horizontal wind speed from (a) Galion VAD scans and (b) WRF simulations. The measured and simulated hourly mean wind profiles for 06:00 on May 14 are presented in (c).

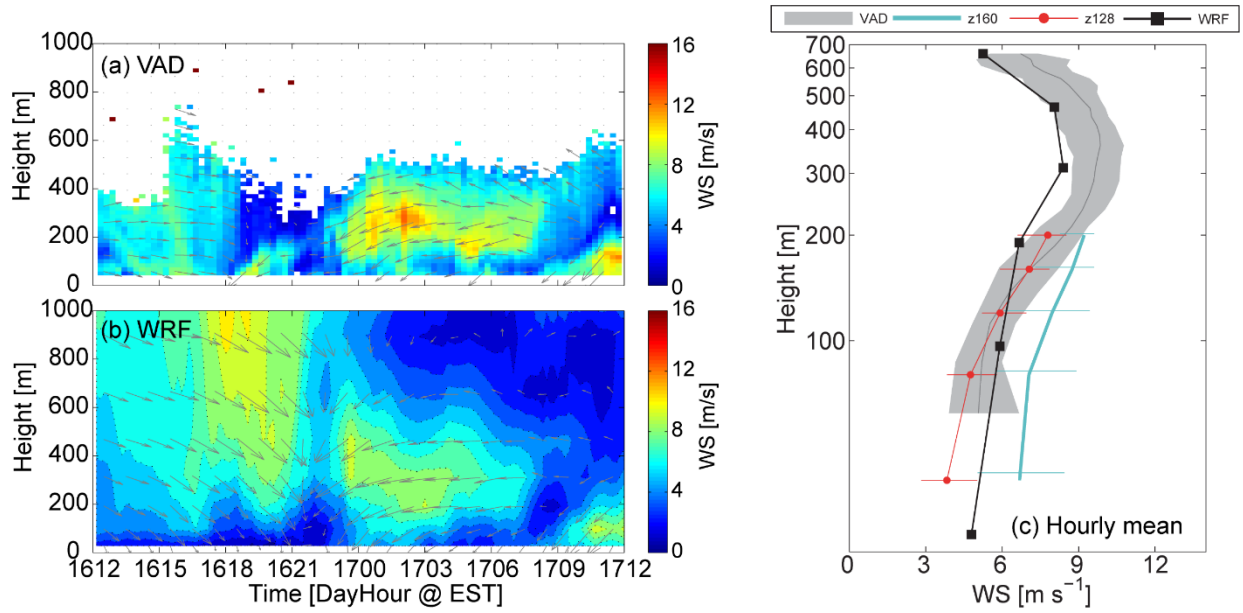

Figure 3.17 Time-height cross sections of wind speed from (a) Galion VAD scans and (b) WRF simulations. The measured and simulated hourly mean wind profiles for 00:00 on May 17 are presented in (c).

3.4.4 Publications and presentations

Doubrawa, P., Barthelmie, R.J., Wang, H., Crippa, P. and Pryor, S.C., 2014: Impacts of boundary condition resolution on numerical simulations of coastal and offshore flow. *American Wind Energy Association Offshore Conference*, October 2014, Atlantic City (Poster).

Barthelmie, R.J., Pryor, S.C., Wang, H. and Doubrawa, P. 2014: Comparison of lidar measurements on the coast of Lake Erie. *American Wind Energy Association Offshore Conference*, October 2014, Atlantic City.

Wang, H., Barthelmie, R.J., Crippa, P., Doubrawa Moreira, P., Pryor S.C. 2014: Profiles of wind and turbulence in the coastal atmospheric boundary layer of Lake Erie, *The Science of Making Torque from Wind*, Lyngby, June 2014. http://iopscience.iop.org/1742-6596/524/1/012117/pdf/1742-6596_524_1_012117.pdf

3.5 Experiment #4 PEIWEE: Prince Edward Island Wind Energy Experiment

3.5.1 Experimental description

3.5.1.1 Objective

Assessing potential costs and benefits of siting wind turbines on escarpments is challenging, particularly when the upstream fetch is offshore leading to more persistent wind speeds in power producing classes, but an increased importance of stable stratification under which terrain impacts on the flow may be magnified. In part because of a lack of observational data, critical knowledge gaps remain and there is currently little consensus regarding optimal models for flow characterization and turbine design calculations.

The two primary objectives of PEIWEE were to; a) Quantify wind energy relevant flow parameters at/behind a coastal escarpment b) Quantify wind turbine wake behavior in complex coastal environments. The Cornell team also had a secondary objective focused error quantification and reduction for lidar retrieval of wind speeds (both mean and higher moments - specifically variance).

3.5.1.2 Site

Experiment location: Wind Energy Institute of Canada (WEICan) on the northern tip of Prince Edward Island (Figure 3.18). The central coordinates are approximately 47.048N 64.00 W in UTM Zone 20, 424043E, 5210983 N (Figure 3.19 and Figure 3.20). This site has many advantages when seeking to develop a unique data set comprising in situ and remote sensing observations of flow parameters over a 10–14 m escarpment at wind turbine relevant heights (from 9 to 200 m). For example it has a long offshore fetch in most directions, there is an IEC Class 2 wind resource with relatively low turbulence and it has infrastructure on site including instrumented tall mast and accommodation for scientists and technicians. There are also a number of large and small wind turbines providing an ideal test bed. A diverse range of field-based studies can be envisaged with goals ranging from wind and turbulence measurements to development and testing of control algorithms and integrating battery storage. In addition, the cliff edge provides an excellent opportunity to study flow in complex terrain (Figure 3.19).

3.5.1.3 Timeline

The dates for the field intensive are May 9-28 2015.

3.5.1.4 Layout and conditions during the experiment

After a short period of co-location for an instrument closure experiment, the lidars and sonic anemometers were deployed close to the IEC standard meteorological mast at a small wind farm at the coast to measure the freestream and wind turbine wakes and coastal flow. See locations shown in Figure 3.18-3.20 and listed in Table 3.8.

Table 3.8 Locations of the wind turbines (T1-T5), the IEC-compliant meteorological mast (MET) on which we deployed three sonic anemometers, the scanning Doppler lidar (Galion) the three ZephIR units (Z125, Z423, Z447) and the short (18-m) meteorological mast on which we deployed a fourth Gill sonic anemometer (M18).

Description	Y (UTM Northing) **m**	X (UTM Easting) **m**
T1	5210290	423140
T2	5209900	422990
T3	5209657	422835
T4	5209401	422602
T5	5208756	422915
MET	5208971	422828
Galion	5208754	422934
Z125	5209326	422769
Z423	5209526	422903
Z447	5209424	422544
M18	5209431	422543

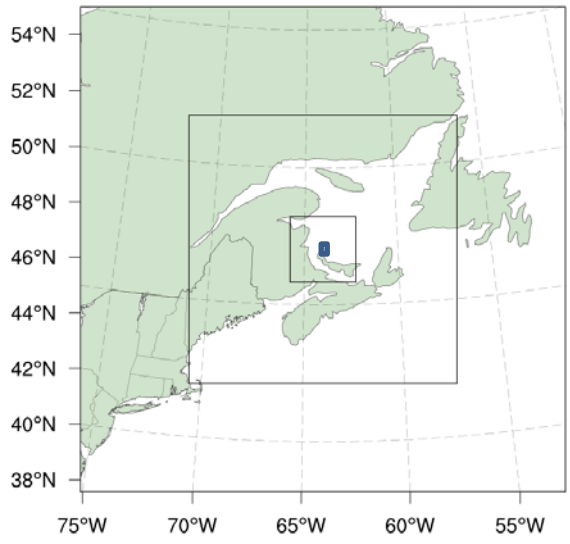

Figure 3.18 Location of WEICAN on the northern tip of Prince Edward Island (PEI) (shown by the blue box) and the domains used for the WRF modeling.

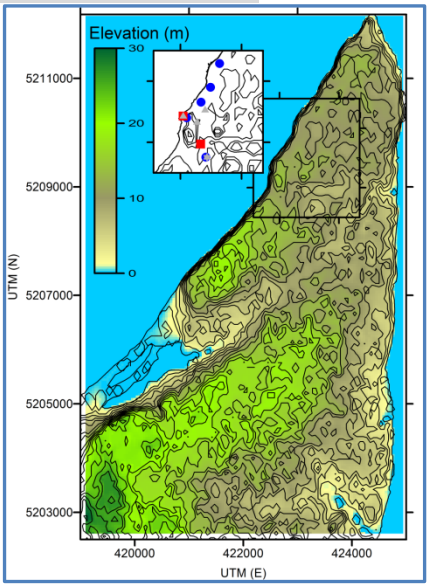

Figure 3.19 Map of the terrain elevation on the northern tip of Prince Edward Island and an inset showing the location of the five wind turbines (shown in blue dots). Wind turbine hub-height=80 m, rotor diameter=93m.

Figure 3.20 Google maps image showing the wind turbines (T1-5), and deployment locations of the 3 ZephIR units (Z125 from WEICan, Z423 and Z447), The meteorological mast (MM) on which three Gill sonic anemometers were deployed (G1-3), the short mast on the coast on which a fourth Gill sonic anemometer was deployed (G4) and the location of the scanning doppler lidar (Galion) that was deployed near the base of T5.

3.5.1.5 Instrumentation deployed and configuration

Table 3.9. Overview of instrumentation deployed by Cornell during PEIWEE and measurement protocols

Pulse scanning lidar (Galion)	1	Primary measurement: Line of sight velocity. Maximum range during experiment: 2 km Derived variables: Horizontal wind speed and direction (turbulence intensity, specific periods). Data integration period: 10 minute Multiple scan patterns employed (Table 3.10)
Continuous wave vertically-pointing Doppler lidars (ZephIR 300 units from Cornell, plus one 150 unit from WEICan)	2	Wind speed, wind direction and turbulence intensity: Heights (m): 20:200:20 Data integration period: 10-minute mean values
Gill WindMaster Pro 3-D sonics	4	u, v, w, T at 10 Hz 20, 40 and 60 m on MM 18 m on coastal jack-up tower

Table 3.10 Detailed scan patterns employed with the Galion lidar (AZ = azimuth angle ° from N, EL = elevation angle ° from ground, FOCAL = focal length (m), MAX RANGE = max. range from which Doppler shift was sought (km), BEARING = bearing ° of instrument from N). Note: Included offset in Galion operating protocol so all data are aligned to N.

NO	SCAN NAME	START_TIME (UTC)	END_TIME (UTC)	DESCRIPTION
1	VAD	2015-05-09 21:00	2015-05-11 12:00	VAD only • AZ: 0:30:330 • EL: 26.388 • FOCAL: 500 • MAX RANGE: 2 • BEARING: 180
2	WAKE_T5_6STACKS	2015-05-11 19:00	2015-05-15 12:00	PPI: • AZ: 304.5:2:34.5 • EL: 1.2:2:11.2 VAD: • AZ:4.5:30:334.5 • EL: 45 Both: • FOCAL: 800 • MAX RANGE: 2 • BEARING: 244
3	WAKE_T5_6STACKS	2015-05-15 13:00	2015-05-17 13:00	PPI: • AZ: 304.5:2:34.5 • EL: 2:2:12 VAD: • AZ:4.5:30:334.5 • EL: 45 Both: • FOCAL: 800 • MAX RANGE: 2 • BEARING: 265
4	STAR_T5_4BEAMS	2015-05-17 13:52	2015-05-19 12:31	Stare scan: • AZ: 333 • EL: 4.8,10,15.2,20.6 • FOCAL: 500 • MAX RANGE: 0.72 • BEARING: 265
5	WAKE_T5_8STACKS WITH FREESTREAM	2015-05-19 13:00	2015-05-25 12.30	VAD: • AZ:34.5:30:304.5 • EL: 60 PPI_1: • AZ: 34.5:2:304.5 • EL: 2:2:12 PPI_2: • AZ: [34.5,24.5,14.5,4.5,354.5:-6:324.5,314.5,304.5] • EL:13.8, 18.2 All: • FOCAL: 500 • MAX RANGE: 0.72 • BEARING: 265
6	NEAR-WAKE	2015-05-25	2015-05-26	PPI_1:

	WITH FREESTREAM	12.57	12.57	• AZ: 15:2:75 • EL:2.9,5,7,9,11.1,12.8,15.3,18.9 PPI_2: • AZ: 195:10:255 • EL: 11.5,15,24.4 Both: • FOCAL: 500 • MAX RANGE: 0.72 • BEARING: 265
7	NEAR-WAKE WITH FREESTREAM	2015-05-26 12.57	2015-05-27 11.15	PPI_1: • AZ: 335:-2:65 • EL:2.9,5,7,9,11.1,12.8,15.3,18.9 • FOCAL: 500 • MAX RANGE: 0.72 • BEARING: 265

3.5.1.6 Numerical simulations

In support of the measurements, WRF simulations were conducted using two-way nesting on three domains of 9, 3 and 1 km horizontal resolution and 61 vertical levels from the surface to 60 hPa, with 10 levels below 200 m. The model was initialized with 12 km North American Mesoscale Forecast System data and sea surface temperatures from National Centers for Environmental Prediction real-time analyses ($0.083 \times 0.083°$). The simulations used WSM 6-class microphysics, rapid radiative transfer model for longwave and Dudhia for shortwave radiation, Monin Obukhov (Eta) surface layer, Noah land surface model and MYNN 2.5 level TKE for boundary layer. The output from these simulations were used as lateral boundary conditions for microscale modeling designed to evaluate the extent of the zone impacted by the escarpment, undertaken in the WAsP family of models. WAsP BZ is a linearized model where analytical solutions are applied to determine terrain corrections to the flow derived as perturbations in the inner, intermediate and outer layers using a length scale (related to the horizontal and vertical dimensions of the terrain feature and to the roughness length). WAsP BZ uses a Bessel function to moderate the terrain perturbations allowing a much greater concentration of contours at the grid center with decreasing resolution moving outwards. Such linear flow models cannot resolve flow detachment and recirculation and tend to over-estimate topographic speed-up under neutral conditions. WAsP computational fluid dynamics (CFD) is designed as an extension of WAsP BZ and specifically to enhance the applicability of the model to complex terrain. It is based on the EllipSys finite volume CFD solver, and the 3D grid is generated by the hyperbolic grid generator. Speed-up ratios are calculated using incompressible Navier–Stokes equations for directional sectors on a fine mesh over a microscale area nested within the WAsP simulation domain. Within the WAsP CFD simulations turning of the wind because of the Coriolis effect and non-neutral stability are neglected. Turbulence deriving from terrain impacts is simulated in WAsP CFD using the two-equation k-ε RANS model. It thus represents an example of a type of model that performed relatively well for the Bolund test case.

3.5.1.7 Participating institutions

Cornell University, WEICan, York University, Western University and the Danish Technical University.

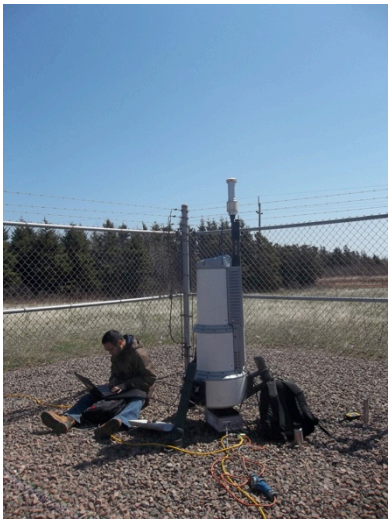

Figure 3.21. Photographs from the experiment at the Wind Energy Institute of Canada showing the turbine locations at the escarpment (left) the IEC compliant meteorological mast with a wind turbine 500 m from the coast where the Galion was located (below left) the ZephIR (operated by the Wind Energy Institute of Canada, below right).

3.5.2 Major results

Measurements collected at WEICan were used to improve fundamental understanding of the flow (and wake behavior) and to evaluate simulations using the EllipSys finite volume CFD model. Comparison of instrument performance in the marine environment showed good agreement for the lidar and mast measured wind speeds plus comparison of observations with model simulations with WAsP, WAsP CFD, WAsP Engineering and WRF were conducted examining flow over the escarpment and an evaluation of the WRF wind farm module.

Flow at coastal escarpments: Results of analyses of data and simulations conducted by the Cornell team indicate good agreement between the observations and WAsP-CFD in terms of the wind speed decrease before the terrain feature and the increase at (and downwind of) the escarpment of ~3–5% at turbine hub-heights. However, the horizontal extent of the region, in which the impact of the escarpment on the mean flow is evident, is larger in the models than the measurements (Figure 3.22). A region of high turbulence was indicated close to the escarpment that extended through the nominal rotor plane, but the horizontal extent of this region was narrow (<10 times the escarpment height, H) in both models and observations. Moving onshore the profile of turbulence was more strongly influenced by higher roughness of a small forest. While flow angles close to the escarpment were very complex, by a distance of 10 H, flow angles were <3° and thus well within limits indicated by design standards (Barthelmie et al. 2016).

Scanning LiDARs offer the potential to provide detailed measurements necessary to characterize wind turbine wakes. We used the Galion scanning doppler lidar to probe wakes from WT at WEICan and then used output from Large-Eddy Simulation (LES) to recreate the LiDAR scanning geometry and estimate the uncertainty when mean wake characteristics are quantified from scanning LiDAR measurements, which are temporally disjunct due to the time that the instrument takes to probe a large volume of air.

Based on LES output, we determine that wind speeds sampled with the synthetic LiDAR are within 10% of the actual mean values and that the disjunct nature of the scan does not compromise the spatial variation of wind speeds within the planes. We propose scanning geometry density and coverage indices, which quantify the spatial distribution of the sampled points in the area of interest and are valuable to design LiDAR measurement campaigns for wake characterization. We find that scanning geometry coverage is important for estimates of the wake center, orientation and length scales, while density is more important when seeking to characterize the velocity deficit distribution (Doubrawa et al. 2016).
The Cornell team also used the data we collected to address issues related to lidar retrieval of wind speeds (both mean and higher moments - specifically variance). The remote sensing community are seeking to extend use of lidar technologies beyond retrieval of mean wind speeds to derive turbulence metrics. A high-fidelity lidar turbulence measurement technique relies on accurate estimates of radial velocity variance. Using data collected with the scanning Doppler lidar we examined the sources of uncertainty in the radial variance. During the experiment, a Galion lidar was configured with 20 kHz pulse repetition frequency and 1.0 s dwell time to scan at four elevation angles (4.8, 10.0, 15.2, and 20.6 deg) with a fixed azimuth angle of 349 deg such that the 7th range gate of the lidar sampled at 20, 40, 60 m (and 80 m) above the ground where three Gill Windmaster Pro sonic anemometers were installed on an IEC compliant meteorological mast. We show that for current-generation scanning lidars and sampling durations of about 30 min and longer, during which the stationarity assumption is valid for atmospheric flows, the systematic error n radial variance is negligible but the random error exceeds about 10 % (Wang et al. 2016a).

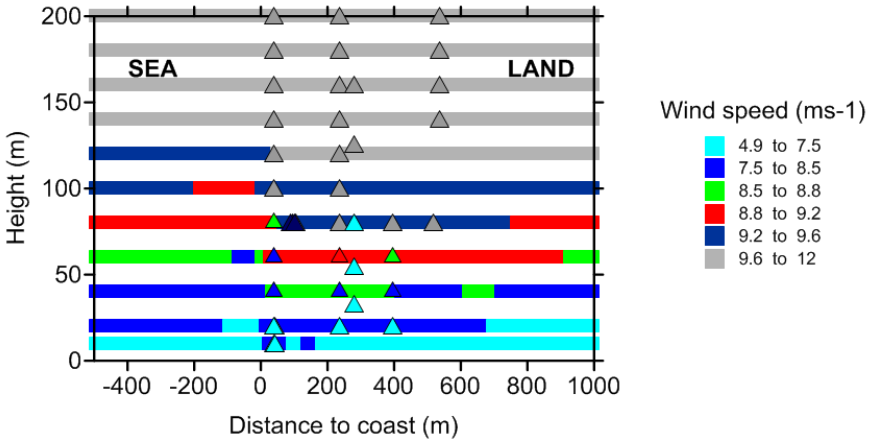

Figure 3.22 Wind speeds in the coastal zone predicted using WasP using Ellipsys CFD for flow perpendicular to the coast of Prince Edward Island (color bands) along with observations (color triangles) from different lidars and a meteorological mast at different distances from the coast.

3.5.3 Publications and presentations

A special session on this experiment was held at the WindTech 2015 conference in October 2015.

Barthelmie, R.J., Doubrawa, P. Wang, H., Giroux, G., Pryor, S.C. 2016: Effects of an escarpment on flow parameters of relevance to wind turbines, *Wind Energy* 19, 2271-2286.

Barthelmie, R.J., Doubrawa, P., Wang, H. and Pryor, S.C. 2016: Defining wake characteristics from scanning and vertically pointing full-scale lidar measurements. *Science of Making Torque from Wind*, Munich, 5-7 October 2016 8 pp.

Wang, H., Barthelmie, R.J., Doubrawa, P. and Pryor, S.C. 2016: Errors in radial velocity variance from Doppler wind lidar**,** *Atmospheric Measurement Techniques*, 9, 4123-4139. doi:10.5194/amt-9-4123-2016.

Doubrawa, P., Barthelmie, R.J., Wang, H., Pryor, S.C. and Churchfield, M. 2016: Wind Turbine Wake Characterization from Temporally Disjunct 3-D Measurements, *Remote Sensing*, 8, 939; doi:10.3390/rs8110939

4 Brief summary of major results

Major findings of our research are:

- Lidar operation:
    - Comparison of instrument performance at a major land-based wind farm indicated good instrument closure (Barthelmie et al. 2014). Further, data we collected in the marine environment at Prince Edward Island showed good agreement for measured wind speeds from the scanning Doppler lidar and vertically pointing lidar with data from mast-mounted sonic anemometers. There was also good agreement between these observations and model simulations with WAsP, WAsP CFD, WAsP Engineering and WRF (Barthelmie et al. 2016). However, epistemic uncertainty (i.e. scientific uncertainty due to lack of process-level understanding) and aleatory uncertainty (arising from random effects and often characterized by alternative models) remain.
    - When applying 3D scanning lidar, use of small azimuth angle PPI's (< 15 degree) leads to large uncertainty in retrieved wind fields and thus such scans are of less value than wider PPI scans. Changing the scanning geometry frequently makes it difficult to process and integrate data over an entire experiment. Our final scanning strategy using an optimized stack of 5 or 6 PPI's with approximately 90 degree arc-width, followed by a VAD scan with a high elevation angle, and a slow RHI roughly into the mean wind direction enables a scan to be completed within 10 minutes with good horizontal and vertical resolution in three dimensions. Based on data from the four field experiments we advanced a new methodology to estimate *a priori* the uncertainty in wind speed retrievals from arc scans based on site characteristics such as wind velocity, turbulence intensity and proposed scan geometry (Wang et al. 2016b). Additional considerations when optimizing scan geometry include the maximum range from which robust Doppler shift information can be obtained. This is a strong function of local aerosol sources.
    - For current-generation scanning Doppler lidars and sampling durations of about 30 min and longer, during which the stationarity assumption is valid for atmospheric flows, the systematic error in radial variance derived from scanning Doppler lidars is negligible but the random error exceeds about 10 % (Wang et al. 2016a).
- Flow in the offshore and coastal environment:
    - Experimental data collected during the Lake Erie campaign indicated a highly non-uniform spatial wind speed distribution (~60% variation) that was enhanced when stability conditions differed between land and lake. We further found the frequent presence of upward momentum and resulting distortion of the wind speed profile at turbine relevant heights due to swells in the Great Lake. A number of periods were characterized by very low wind shear including hours with near-zero wind shear and low level jets at 600 m height over the Lake which were captured by the WRF model simulations.
    - Experimental data and modeling of our experiment at WEICAN showed that a 10-14 m escarpment adjacent to long-overseas fetch causes a zone of wind speed decrease before the terrain feature and that the wind speed increase at (and slightly downwind of) the escarpment is ~3–5% at turbine hub-heights. While flow angles close to the escarpment were very complex, flow angles at 200 m inland were <3° and thus well within limits indicated by design standards.
- Wind turbine wakes:
    - Scanning LiDARs offer the potential to provide detailed measurements necessary to characterize wind turbine wakes. We used the scanning Doppler lidar to probe wakes and quantify their length and velocity scales. Combined with output from Large-Eddy Simulation (LES), we determine that wind speeds sampled with the synthetic LiDAR are within 10% of the actual mean values and that the disjunct nature of the scan does not compromise the

spatial variation of wind speeds. Scanning geometry coverage is important for estimates of the wake center, orientation and length scales, while density is more important when seeking to characterize the velocity deficit distribution (Doubrawa et al. 2016).

  - Observations of wakes using the lidars (vertically pointing and scanning) and from mast-deployed anemometers indicate that directly downstream of a turbine (at a distance of 190 m, or 2.4 rotor diameters (D)), there is a clear impact on wind speed and turbulence intensity (TI) throughout the rotor swept area. However, at a downwind distance of 2.1 km (26 D downstream of the closest wind turbine) the wake of the whole wind farm is not evident (Smith et al. 2013).

- In a broader context, we also supported graduate students, gave 60 conference presentations and published 14 papers in international research journals. We published a new Wind Atlas for the Great Lakes from integration of remote sensing data, in situ measurements, reanalysis products and numerical models to generate low error wind fields (Doubrawa et al. 2015). We examined how the cost of offshore wind turbine deployments is related to factors such as the distance of the wind farm to the coast and its size (Sovacool et al. 2017). We proposed a new more accurate model for use in the standards (IEC 61400-3-1 ED1) relating to turbulence in the offshore environment (Wang et al. 2014a). We showed implementation of moderate wind energy scenarios can have a meaningful impact on reducing greenhouse gases emissions delaying crossing the 2°C warming threshold by 1–6 years or with a more aggressive implementation avoids passing this threshold altogether (Barthelmie and Pryor 2014).

5 Future work

While significant progress was achieved in the project, further work is urgently needed to:

- Generate further high-quality observational data sets in challenging areas such as the coastal zone, offshore, complex and forested terrain to enhance understanding of flow conditions of relevance to the wind energy community and for model development and evaluation. There remains significant uncertainty in resource assessment, not least because current wind turbines are largely in the 3MW+ capacity with associated hub-heights and rotor diameters that exceed 100 m. Understanding wind and turbulence profiles above the surface layer (often approximately 100 m) requires further research, particularly where stability effects are difficult to determine and wind speed profiles are not likely to average out to approximate a near-logarithmic profile or to frequently deviate from that profile.
- Improve understanding of how wind turbines interact with the atmosphere in large wind farms particularly those deployed in large arrays offshore and in complex terrain. One of the major outstanding questions for wind farm development relates to optimum spacing of wind turbines and/or micro-siting. In many cases, the impact of wakes on turbine performance are significant both in terms of power and loads. However, there are very few available databases to assist in improving wake modeling and it is desirable to obtain new experimental data.
- Improve characterization and best practice for use of lidar for wind energy applications. The major advantage in the use of lidar is that flow can be characterized over large volumes on scales that are relevant not just for single wind turbines but also up to the size of large wind farms. Opportunities for integrating lidar datasets are expanding beyond resource assessment and wake characterization and into the areas of design and control. Design of field experiments and processing of lidar data is far from trivial, not least because of the different types of lidar, their spatial and temporal characteristics and the flow characteristics that can be generated with the required accuracy. Further work in the optimization of lidar scanning will result in reduced expense of lidar campaigns and lower uncertainty in resulting flow characterization. Further work in developing processing tools will assist in enabling more widespread use of lidar in many wind-related applications. Both are needed if the full potential of lidar is to be realized in the continuing effort to keep wind energy prices low with expansion into more challenging areas (notably offshore and complex, forested terrain).

6 Products and news stories

6.1 Refereed journal papers

1) Sovacool, B, Enevoldsen, P, Koch, C. and Barthelmie, R.J. 2017: Cost performance and risk in the construction of offshore and onshore wind farms, Wind Energy, 20, 891–908
2) Doubrawa, P., Barthelmie, R.J. and Churchfield, M. 2017: A stochastic wake model based on new metrics for wake characterization, Wind Energy, 20, 449–463
3) Wang, H., Barthelmie, R.J., Doubrawa, P. and Pryor, S.C. 2016: Errors in radial velocity variance from Doppler wind lidar, Atmospheric Measurement Techniques, 9, 4123-4139.
4) Barthelmie, R.J., Doubrawa, P. Wang, H., Giroux, G., Pryor, S.C. 2016: Effects of an escarpment on flow parameters of relevance to wind turbines, Wind Energy, 19, 2271-2286
5) Doubrawa, P., R. J. Barthelmie, H. Wang, S. C. Pryor, and M. Churchfield, 2016: Wind turbine wake characterization from temporally disjunct 3-D measurements. Remote Sensing, 8, 939; doi:10.3390/rs8110939
6) Wang, H., Barthelmie, R.J., Pryor, S.C. and Brown, G.: 2016 Lidar arc scan uncertainty reduction through scanning geometry optimization, Atmospheric Measurement Techniques, 9, 1653–1669
7) Wang, H., Barthelmie R.J., Clifton, A. and Pryor S.C. 2015: Wind measurements from arc scans with doppler wind lidar, Journal of Atmospheric and Oceanic Technology, 32, 2024-2040.
8) Doubrawa, P., Barthelmie, R.J. Hasager, C.B., Badger, M., Karagali, I. and Pryor, S.C. 2015: Satellite winds as a tool for offshore wind energy resource assessment: The Great Lakes Wind Atlas, Remote Sensing of the Environment, 168, 349-359.
9) Barthelmie, R.J. and Pryor S.C. 2014: The potential contribution of wind energy to climate change mitigation. Nature Climate Change, 4, 684-688.
10) Barthelmie, R.J., Crippa, P., Wang, H., Smith, C.M., Krishnamurthy, R., Choukulkar, A., Calhoun, R., Valyou, D., Marzocca, P., Matthiesen, D., Brown, G. and Pryor, S.C. 2013: 3D wind and turbulence characteristics of the atmospheric boundary-layer. Bulletin of the American Meteorological Society, 95, 743–756.
11) Smith, C.M., Barthelmie, R.J. and Pryor, S.C. 2013: In situ observations of the influence of a large onshore wind farm on near-surface temperature, turbulence and wind speed profiles. Environmental Research Letters, 8, 034006 .
12) Wang, H., Barthelmie, R.J., Pryor, S.C. and H.G. Kim 2013: A new turbulence model for offshore wind turbine standards, Wind Energy, 17, 1587-1604.
13) Barthelmie, R.J. and Pryor, S.C. 2013: Wake model evaluation using data from the Virtual Wakes Laboratory, Applied Energy, 104, 834-844.
14) Barthelmie, R.J., Hansen, K.S. and Pryor, S.C. 2013: Meteorological controls on wind turbine wakes, Marine Energy and Environments. Invited Paper. Special Issue Proceedings of the Institute Electrical and Electronics Engineers, 101(4), 1010-1019.

6.2 Conference papers and presentation

*Reports listed have permanent accessibility

1. Barthelmie, R.J., Doubrawa, P., Wang, H. and Pryor, S.C. 2016: Defining wake characteristics from scanning and vertically pointing full-scale lidar measurements. *Science of Making Torque from Wind*, Munich, 5-7 October 2016. Journal of Physics: Conference Series 753 (2016) 032034 doi:10.1088/1742-6596/753/3/032034.
2. Doubrawa, P., Barthelmie, R.J., Wang, H., Churchfield, M.J. 2016: Contributions of the Stochastic Shape Wake Model to Predictions of Aerodynamic Loads and Power under Single Wake Conditions, *Science of Making Torque from Wind*, Munich, 5-7 October 2016. Journal of Physics: Conference Series **753** (2016) 082006 doi:10.1088/1742-6596/753/8/082006.
3. Barthelmie, R.J. 2016: *Quantifying wind turbine wakes with measurements,* Affiliate Professor Inaugural lecture, August 3 2016, Danish Technical University, Risø campus.

4. Barthelmie, R.J., Wang, H., Doubrawa, P. and Pryor, S.C. 2016: Best Practice for Measuring Wind Speeds and Turbulence Offshore through In-situ and Remote Sensing Technologies, Report to Department of Energy. DE- EE0005379. 7 July 2016. 47 pp. http://doi.org/10.7298/X4QV3JGF
5. Barthelmie, R.J. and Pryor, S.C. 2016: Flow and wakes in complex terrain: Results from the Prince Edward Island Experiment, *European Academy of Wind Energy Ph.D. seminar,* Invited speaker, May 24-25 2016, Danish Technical University, Lyngby
6. Pryor, S.C. and Barthelmie, R.J. 2016: Can/will climate change impact the wind energy industry? *ICRC-CORDEX 2016*, Stockholm.
7. Doubrawa, P., Barthelmie, R.J., Wang, H., Pryor, S.C. and Churchfield, M.C. 2016: Wind Turbine Wake Characterization Metrics for Temporally Disjunct 3D Measurements. *ISARS2016, 18th International Conference for the advancement of boundary-layer remote sensing*, Varna, Bulgaria 6-9 June 2016.
8. Barthelmie, R.J., Wang, H., Doubrawa, P. and Pryor, S.C. 2016: Quantifying full-scale wakes with lidar measurements. *ISARS2016, 18th International Conference for the advancement of boundary-layer remote sensing*, Varna, Bulgaria 6-9 June 2016 (Poster).
9. Barthelmie, R.J., Wang, H., Doubrawa, P. and Pryor, S.C. 2016: Measuring wakes with lidar. Panel presentation *2016 Wind Energy Research Workshop*, Lowell, MA on March 15-16 2016.
10. Barthelmie, R.J., Doubrawa, P., Wang, H., and Pryor, S.C. 2016: Observations and simulations of flow over an escarpment. 2*016 Wind Energy Research Workshop*, Lowell, MA on March 15-16 2016.
11. Barthelmie, R.J. 2016: Wind Energy Success: What Next? Invited keynote presentation to WindSTAR banquet, February 8 2016, University of Texas at Dallas.
12. Pryor, S.C. and Barthelmie, R.J. 2016: Can/will climate change impact the wind energy industry? Climatic Research Unit/Environmental Sciences Seminar, University of East Anglia, January 12 2016.
13. Hasager, C.B., Madsen, P.H., Giebel, G., Réthoré, P.E., Hansen, K.S., Badger, J., Peña, A., Volker, P., Badger, M., Karagali, I., Cutulusis, N., Maule, P., Schepers, G. Wiggelinkhuizen, E.J., Cantero, E., Waldl, I., Anaya-Lara, O., Attya, I., Svendsen, H., Palomares, A., Palma, J., Costa Gomes, V., Gottschall, J., Wolken-Möhlmann, G., Bastigkeit, G., Beck, H., Trujillo, J.J., Barthelmie, R.J., Sieros, G., Chaviaropoulos, T., Vincent, P., Husson, H., Prospathopoulos, J. 2015: Design tool for offshore wind farm cluster planning, *European Wind Energy Conference*, Paris, November 2015, 10 pp.
14. Barthelmie, R.J., Wang, H., Doubrawa, P. and Pryor, S.C. 2015: An overview of the PEIWEE experiment 2015, *WindTech 2015*, Western University, Ontario, October 19-21 2015. (Invited keynote)
15. Wang, H., Barthelmie, R.J., Doubrawa, P. and Pryor, S.C. 2015: Uncertainty in Doppler Lidar Radial Velocity Variance Measurements, *WindTech 2015,* Western University, Ontario, October 19-21 2015.
16. Barthelmie, R.J., Wang, H., Doubrawa, P. and Pryor, S.C. 2015: Wind Turbine Wakes from Scanning Lidar, *WindTech 2015*, Western University, Ontario, October 19-21 2015.
17. Doubrawa, P., Wang, H., Pryor, S.C. and Barthelmie, R.J. 2015: WRF Simulations of a Pseudo Offshore Wind Farm: Validation Against Field Measurements and Evaluation of Wind Turbine Drag Parameterization, *WindTech 2015*, Western University, Ontario, October 19-21 2015.
18. Pryor, S.C. , Wang, H., Doubrawa, P. and Barthelmie, R.J. Measurements and Modeling of Wind Turbine Relevant Flow Parameters at an Escarpment During PEIWEE. *WindTech 2015*, Western University, Ontario, October 19-21 2015.
19. Barthelmie, R.J. 2015: Flow in complex terrain at height relevant to wind energy. *Seminar in Atmospheric Science Graduate Field*, Cornell University, 24 September 2015.
20. Barthelmie, R.J. 2015: Offshore wind energy; perspectives and prospects. *Offshore Energy and Storage Symposium*-3 July 2015, Edinburgh, UK

21. Barthelmie, R.J. (2015) Offshore wind energy; perspectives and prospects. *Offshore Energy and Storage Symposium*-3 July 2015, Edinburgh, UK
22. Wang, H., Barthelmie, R.J., Pryor, S.C. and Brown, G. 2015: Uncertainty in lidar arc scan measurement, *IEA Wind Topical Expert Meeting, #82 on Uncertainty Quantification of Wind Farm Flow Models*, June 12 2015, Visby, Sweden.
23. Wang, H. and Barthelmie, R.J. 2015: Wind turbine wake detection with a single Doppler wind lidar, *Wake Conference*, Visby, Sweden, 9-10 June 2015. 9 pp. Journal of Physics: Conference Series **625** 012017 doi:10.1088/1742-6596/625/1/012017
24. Barthelmie, R.J. Churchfield, M.J., Moriarty, P.J., Lundquist, J.K., Oxley, G.S, Hahn, S. and Pryor, S.C. 2015: The role of atmospheric stability/turbulence on wakes at the Egmond aan Zee Offshore wind farm, *Wake Conference*, Visby, Sweden, 9-10 June 2015. 10 pp. Journal of Physics: Conference Series 625 012002 doi:10.1088/1742-6596/625/1/012002
25. Doubrawa, P., Barthelmie, R.J., Wang, H., Pryor, S.C. and Badger, M. 2015: Quantifying the Impact of Assuming Neutral Atmospheric Stratification in the Integration of Remote Sensing and In Situ Data Into a Wind Atlas for Lake Erie, *American Geophysical Union Spring Meeting*, Boston, May 2015.
26. Doubrawa, P., Barthelmie, R.J., Wang, H., Crippa, P. and Pryor, S.C., 2014: Impacts of boundary condition resolution on numerical simulations of coastal and offshore flow. *American Wind Energy Association Offshore Conference*, October 2014, Atlantic City (Poster).
27. Barthelmie, R.J., Pryor, S.C., Wang, H. and Doubrawa, P. 2014: Comparison of lidar measurements on the coast of Lake Erie. *American Wind Energy Association Offshore Conference*, October 2014, Atlantic City.
28. Doubrawa, P., Barthelmie, R.J., Badger, M., Karagali, I. and Hasager, C.B., 2014: Wind resource assessment of the Great Lakes from in situ and remote sensing observations. *American Wind Energy Association Offshore Conference*, October 2014, Atlantic City (Poster).
29. Barthelmie, R.J. and Pryor, S.C. 2014: Potential measurement strategy with lidar and sonics: Opportunity and issues, *Microscale modeling of complex terrain flows*, 25-26 September, University of Notre Dame.
30. Barthelmie, R.J. and Pryor, S.C. 2014: The potential of wind energy in climate change mitigation, *Energy Engineering Seminar Series*, September 2014, Cornell University.
31. Pryor, S.C. and Barthelmie, R.J. 2013: Can climate change impact wind energy? *The science of making torque from wind conference*, June 2014, Lyngby, Denmark (Poster).
32. Wang, H., Barthelmie, R.J., Crippa, P., Doubrawa Moreira, P. 2014: Observations of Coastal Atmospheric Boundary Layer over Lake Erie, *The Science of Making Torque from Wind*, Lyngby, June 2014. http://iopscience.iop.org/1742-6596/524/1/012117/pdf/1742-6596_524_1_012117.pdf
33. Barthelmie, R.J. and Pryor, S.C. 2013: Can wind energy impact climate change? *The science of making torque from wind conference*, June 2014, Lyngby, Denmark (Invited keynote).
34. Barthelmie, R.J. 2014: Wind energy 2030. Distinguished Faculty Research Lecture Indiana University (sole annual recipient), Indiana University, 2 April 2014.
35. Barthelmie, R.J. 2014: Everything you wanted to know about wind energy but were afraid to ask. Invited Keynote Presentation at the *Crossroads Geology conference*, Indiana University, March 28 2014.
36. Barthelmie, R.J., Doubrawa Moreira, P, Badger, M. and Hasager, C.B. 2014: Satellite and ground based observations integrated into a wind atlas for the Great Lakes, *European Wind Energy Association Conference*, Barcelona, March 2014 (Poster #170).
37. Barthelmie, R.J., Wang, H. and Pryor, S.C. 2014: Measuring full scale wind turbine wakes, *European Wind Energy Association Conference*, Barcelona, March 2014.
38. Barthelmie, R.J., Pryor, S.C. and Wang, H. 2013: 3D Wind: Quantifying wind and turbulence intensity. *American Geophysical Union Fall Meeting*, San Francisco, 9-13 December 2013 (Poster A13G-0309).

39. Wang, H., Barthelmie, R.J., Clifton, A., Capaldo, N. and Pryor, S.C. 2013: 3D wind: Developing and testing wind velocity retrieval algorithms for Doppler wind lidar #1798284. *American Geophysical Union Fall Meeting,* San Francisco, 9-13 December 2013 (Poster A13G-0304).
40. Barthelmie, R.J., Wang, H. and Pryor, S.C. 2013: Wind resource and wakes- results from the 3D wind experiment. *European Offshore Wind Energy Conference and Exhibition,* Frankfurt, November 2013.
41. Barthelmie, R.J., Pryor, S.C., Hansen, K.S. and Macguire, E. 2013: Wake merging at Lillgrund. *European Offshore Wind Energy Conference and Exhibition,* Frankfurt, November 2013.European Offshore Wind Energy Conference. Poster Prize (one of three non-student prizes).
42. Barthelmie, R.J.. 2013: Field experiment approaches to wind resource and wakes. *WindEEE Scientific Symposium,* 16 October 2013.
43. Barthelmie, R.J., Wang, H. and Pryor, S.C. 2013: Wind resource and wakes- results from the 3D wind experiment. *Invited presentation at International Conference on Future Technologies for Wind Energy,* 7-9 October 2013.
44. D. Valyou, P. Marzocca, A. Ceruti, "Design, performance and flight operation of an all composite unmanned aerial vehicle." *SAE 2013 AeroTech Congress & Exhibition,* September 24-26, 2013, Montreal, Canada.
45. Ceruti, D. Valyou, P. Marzocca "An integrated software environment for UAV mission operations." *SAE 2013 AeroTech Congress & Exhibition*, September 24-26, 2013, Montreal, Canada.
46. Grappasonni, M. Arras, G. Coppotelli, J.T. Miller, D.N. Valyou, P. Marzocca, "System identification from GVT and taxing of an unmanned aerial vehicle," SAE 2013 AeroTech Congress & Exhibition, September 24-26, 2013, Montreal, Canada.
47. Wang, H., Barthelmie, R.J., Pryor, S.C. and Kim, H.G. 2013: The relationship between wind speed and turbulence intensity for offshore wind turbine design, *North American Wind Energy Academy Conference*, Boulder, August 2013.
48. Barthelmie, R.J., Wang, H. and Pryor, S.C. 2013: Measurement of wind resource and wakes - results and lessons from the 3D wind experiment. *Invited presentation at DONG*, Fredericia, 8 July 2013.
49. Barthelmie, R.J. H. Wang and Pryor S.C. 2013: *An Integrated Approach to Offshore Wind Energy Assessment: Great Lakes 3D Wind Experiment,* X-Wi-Wa Workshop, DTU Risoe, Denmark, 11 June 2013.
50. Barthelmie, R.J. and Pryor, S.C. 2013: Wake model evaluation metrics and the virtual wakes laboratory. *Proceedings of the 2013 International Conference on Aerodynamics of Offshore Wind Energy Systems and Wakes (ICOWES2013),* Lyngby, June 2013, 173-181.
51. Pryor, S.C., Barthelmie, R.J., Crippa, P., Wang, H., Smith, C.M., Krishnamurthy, R., Calhoun, R., Valyou, D., Marzocca, P., Matthiesen, D., and Brown, G. 2013: Great Lakes 3D Wind Experiment. *Proceedings of the 2013 International Conference on Aerodynamics of Offshore Wind Energy Systems and Wakes (ICOWES2013),* Lyngby, June 2013, 132-137.
52. Barthelmie, R.J. 2013: *Wind energy: Status and trends*, IEEE Clean Energy, Case Western Reserve University, May 2013 (invited).
53. Barthelmie, R.J. and Pryor 2012: Wake model evaluation metrics. *IEA Wakebench Annual Meeting,* 9 November 2012, National Renewable Energy Laboratory, Colorado.
54. Barthelmie, R.J. 2012: Great Lakes 3D wind experiment. Part I. Calibration and testing. *IEA Wakebench Annual Meeting,* 8 November 2012, National Renewable Energy Laboratory, Colorado.
55. Smith, C.M., Barthelmie, R.J., Churchfield, M. and Moriarty, P. 2012: Complex wake merging phenomena in large offshore wind farms. *AWEA Offshore,* 9-11 October 2012, Virginia Beach.
56. Pryor, S.C., R.J. Barthelmie, H. Wang 2012: Extreme wind speeds in the coastal and offshore regions of the USA. AWEA Offshore, 9-11 October 2012, Virginia Beach. (Poster).

57. Barthelmie, R.J., S.C. Pryor, C.M. Smith, P. Crippa, H. Wang, Krishnamurthy, R., R. Calhoun, D. Valyou, Marzocca, P., Matthiesen, D. and N. Capaldo 2012: Great Lakes 3D wind experiment. Part I. Calibration and testing. AWEA Offshore 9-11 October 2012 Virginia Beach. (Poster).
58. Smith, C.M., Barthelmie, R.J., Churchfield, M. and Moriarty, P. 2012: Complex wake merging phenomena in large offshore wind farms. American Meteorological Society 20th Symposium on Boundary Layers and Turbulence, Boston, MA, August 2012.
59. Wang, H., Barthelmie, R.J. and Pryor, S.C. 2012: Suitability of offshore wind turbine design standards for America, Asia and Europe. European Wind Energy Conference and Exhibition, Copenhagen, April 2012. (Poster)
60. Barthelmie, R.J., Smith, C.M., Moriarty, P. and Churchfield, M. 2012: Wake merging in large offshore wind farms, European Wind Energy Conference and Exhibition, Copenhagen, April 2012. (Poster)

6.3 Other products

A special session organized on the results of the Prince Edward Island experiment at the WindTech 2 conference held at Western University in October 2015.
Two graduate students (Wang and Doubrawa) and one Post Doc (Smith) participated in the project under the supervision of Professor Barthelmie and were partially supported by this project. Both students have successfully graduated with M.Eng and Ph.D. from Cornell University and one student was supported at Case Western University who graduated with a M.Sc. degree.

6.4 Media

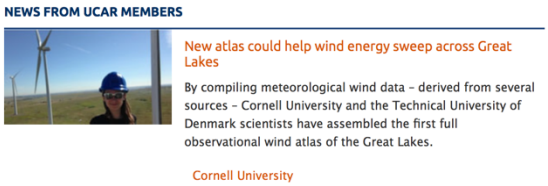

- WindTech October 2015 http://www.windtech-international.com/product-news/news/products-news/new-wind-atlas-could-help-wind-energy-sweep-across-great-lakes
- Wind Atlas story at DTU http://www.vindenergi.dtu.dk/english/News/2015/09/New-Wind-Atlas-for-the-Great-Lakes?id=38cbc7d0-fddb-4943-a737-e85bdef7fd8c&utm_source=newsletter&utm_media=mail&utm_campaign=DTU%20Wind%20Energy%20newsletter%203
- Wind Atlas story on ABC6 news 23 September 2015
- Atlas gives clearer picture of Great Lakes offshore wind potential https://www2.ucar.edu/news/members (September 2015)
- Atlas gives clearer picture of Great Lakes offshore wind potential, http://midwestenergynews.com/2015/09/16/atlas-gives-clearer-picture-of-great-lakes-offshore-wind-potential/
- New atlas could help wind energy sweep across Great Lakes, Cornell Chronicle 8 September 2015, http://news.cornell.edu/print/28021
    - http://news.indiana.edu/releases/iu/2013/12/wind-energy-research-award.shtml
- Clarkson University News: “Clarkson University Researchers Ready Unmanned Aerial Vehicle for DOE Wind Study” 02-01-2012, http://www.clarkson.edu/news/2012/news-release_2012-02-01-1.html

- sUAV News “Research Team from Clarkson University Develops UAV for US DOE Wind Study,” 02-03-2012, http://www.suasnews.com/2012/02/11638/research-team-from-clarkson-university-develops-uav-for-us-doe-wind-study/
- Clarkson University's Unmanned Aerial Vehicle "Golden Eagle" Project, http://www.clarksonuniversityuav.blogspot.com/
- WWNY “Clarkson Develops Drone To Help Build Wind Turbines” 07-07-2012, http://www.wwnytv.com/news/local/Clarkson-Develops-Drone-To-Help-Build-Wind-Turbines-157916925.html
- OffshoreWIND.biz, “Clarkson University Research Team Gets Ready for DOE Wind Study” 02/02/2012, http://www.offshorewind.biz/2012/02/02/clarkson-university-research-team-gets-ready-for-doe-wind-study-usa/
- Unmanned Systems Technologies, “UAV Developed for Wind Speed and Turbulence Analysis,” 06/08/2012, http://www.unmannedsystemstechnology.com/2012/06/uav-developed-for-wind-speed-and-turbulence-analysis/
- Enviro News “UAV Wind Turbine Research Programme Launched,” 02-02-2012, http://www.enviro-news.com/news/uav-wind-turbine-research-programme-launched.html
- Clarkson University UAV Maiden Flight Wide-Angle Camera, 05-16-2016, http://www.youtube.com/watch?v=vlKQQ_5ssTY
- reNEWS Americas Offshore Wind, “Wind resource drone ready for action,” 02-02-2012, http://renewsamericas.com/story.php?page_id=48&news_id=1349
- http://www.apptech.com/photo-contest.html

7 Acknowledgements

Most of the research we conducted involved large multiple-instrument and multi-organization experiments. These experiments are difficult, complicated and time-consuming to organize and run. We gratefully acknowledge the help we received from many corporations, institutes, and individuals who allowed use to use their land (and sometimes their electricity) for this research and helped us with the practicalities, notably the National Renewable Energy Laboratory, the Port Authority of Cleveland, Cleveland Yacht Club and the Wind Energy Institute of Canada. The wind farm in Indiana requested anonymity.

8 Bibliography

Barthelmie, R. J., and S. C. Pryor, 2014: Potential contribution of wind energy to climate change mitigation. *Nature Clim. Change*, **4,** 684-688.

Barthelmie, R. J., P. Doubrawa, H. Wang, G. Giroux, and S. C. Pryor, 2016: Effects of an escarpment on flow parameters of relevance to wind turbines. *Wind Energy*, **19,** 2271-2286.

Barthelmie, R. J., and Coauthors, 2014: 3D wind and turbulence characteristics of the atmospheric boundary-layer. *Bulletin of the American Meteorological Society*, **95,** 743–756.

Doubrawa, P., R. J. Barthelmie, H. Wang, S. C. Pryor, and M. Churchfield, 2016: Wind turbine wake characterization from temporally disjunct 3-D measurements. *Remote Sensing*, **8,** doi:10.3390/rs8110939.

Doubrawa, P., R. J. Barthelmie, S. C. Pryor, C. B. Hasager, M. Badger, and I. Karagali, 2015: Satellite winds as a tool for offshore wind energy resource assessment: The Great Lakes wind atlas. *Remote Sensing of Environment*, **168,** 349-359.

Smith, C. M., R. J. Barthelmie, and S. C. Pryor, 2013: In situ observations of the influence of a large onshore wind farm on near-surface temperature, turbulence intensity and wind speed profiles *Environmental Research Letters*, **8,** 034006.

Sovacool, B. K., P. Enevoldsen, C. Koch, and R. J. Barthelmie, 2017: Cost performance and risk in the construction of offshore and onshore wind farms. *Wind Energy*, **20,** 891-908.

Wang, H., R. J. Barthelmie, S. C. Pryor, and H. G. Kim, 2014a: A new turbulence model for offshore wind turbine standards. *Wind Energy*, **17,** 1587-1604.

Wang, H., R. J. Barthelmie, A. Clifton, and S. C. Pryor, 2015: Wind measurements from arc scans with Doppler wind lidar. *Journal of Atmospheric and Oceanic Technology* **32,** 2024-2040.

Wang, H., R. J. Barthelmie, P. Doubrawa, and S. C. Pryor, 2016a: Errors in radial velocity variance from Doppler wind lidar. *Atmospheric Measurement Techniques*, **9,** 4123-4139.

Wang, H., R. J. Barthelmie, S. C. Pryor, and G. Brown, 2016b: Lidar arc scan uncertainty reduction through scanning geometry optimization. *Atmos. Meas. Tech.*, **9,** 1653-1669.

Wang, H., R. J. Barthelmie, P. Crippa, P. Doubrawa, and S. C. Pryor, 2014b: Observations of Coastal Atmospheric Boundary Layer over Lake Erie. *Journal of Physics: Conference Series*, **524** 012117.